

**EFFECT OF PULP TYPE ON THE RATES OF DELIGNIFICATION  
AND CELLULOSE DEGRADATION DURING OZONE BLEACHING**

By

Janice E. King

B. Sc., Memorial University of Newfoundland, 1996

A Thesis Submitted in Partial Fulfilment of  
the Requirements for the Degree of

**Master of Science in Engineering**

in the Graduate Academic Unit of Chemical Engineering

Supervisor: A. R. P. van Heiningen, Ph. D., Chemical Engineering

Examining Board: D.H. Lister, Ph.D., Chemical Engineering  
M. Sain, Ph.D., Chemical Engineering  
M. Schneider, Ph.D., Forestry and Environmental Management

THE UNIVERSITY OF NEW BRUNSWICK

May, 2000

© Janice E. King, 2000



National Library  
of Canada

Acquisitions and  
Bibliographic Services

395 Wellington Street  
Ottawa ON K1A 0N4  
Canada

Bibliothèque nationale  
du Canada

Acquisitions et  
services bibliographiques

395, rue Wellington  
Ottawa ON K1A 0N4  
Canada

*Your file* *Votre référence*

*Our file* *Notre référence*

**The author has granted a non-exclusive licence allowing the National Library of Canada to reproduce, loan, distribute or sell copies of this thesis in microform, paper or electronic formats.**

**The author retains ownership of the copyright in this thesis. Neither the thesis nor substantial extracts from it may be printed or otherwise reproduced without the author's permission.**

**L'auteur a accordé une licence non exclusive permettant à la Bibliothèque nationale du Canada de reproduire, prêter, distribuer ou vendre des copies de cette thèse sous la forme de microfiche/film, de reproduction sur papier ou sur format électronique.**

**L'auteur conserve la propriété du droit d'auteur qui protège cette thèse. Ni la thèse ni des extraits substantiels de celle-ci ne doivent être imprimés ou autrement reproduits sans son autorisation.**

0-612-65497-4

**Canada**

***To my family who waited patiently and  
to my friends who believed in me.***

## **ABSTRACT**

The rates of delignification and cellulose degradation are measured for ozonation of several different oxygen delignified hardwood and softwood species. They are Cottonwood, Southern Hardwood, Southern Pine and Hemlock. It is found that the maximum rates of delignification and cellulose degradation occur at a consistency about 10% above the fibre saturation point. The differences between the rates virtually disappear when they are normalized for initial kappa number, ozone pressure, average fibre wall thickness and fibre saturation point using the shrinking core model of lignin removal from the fibre wall by ozone. The rate data generated in this study can be described by generalized delignification and cellulose degradation curves which are solely based on the physical and chemical properties of the pulp and the applied ozone conditions.

## **ACKNOWLEDGEMENTS**

I would like to express my sincerest appreciation to my supervisor Dr. Adriaan van Heiningen for all his advice, knowledge and encouragement throughout this study. His guidance and support has made this work possible.

I would like to thank Dr. R. Turner of the Mathematics and Statistics department for his assistance with data analysis and Quok Foo Lee and Mike Lawlor for their help conducting experiments.

Financial support provided by Union Camp Corporation is greatly appreciated.

## TABLE OF CONTENTS

<b>Dedication .....</b>	<b>ii</b>
<b>Abstract.....</b>	<b>iii</b>
<b>Acknowledgements .....</b>	<b>iv</b>
<b>Table of Contents .....</b>	<b>v</b>
<b>List of Tables .....</b>	<b>vii</b>
<b>List of Figures.....</b>	<b>viii</b>
<b>Nomenclature .....</b>	<b>xi</b>
<b>Chapter 1      Introduction.....</b>	<b>1</b>
1.1 Objective and Strategy .....	2
1.2 Thesis Outline .....	2
<b>Chapter 2      Literature Review .....</b>	<b>4</b>
2.1 Ozone Bleaching Technologies .....	4
2.2 Commercial HC Ozone Bleaching.....	6
2.3 Modelling of Ozone Bleaching Kinetics.....	8
2.4 Chemistry of Delignification and cellulose degradation.....	14
2.5 Fibre Wall Structure.....	16
2.6 Fibre Width Distribution.....	20
2.7 Effect of Consistency .....	21
<b>Chapter 3      Experimental Procedure .....</b>	<b>24</b>
3.1 Experimental Set-up.....	24
3.2 Pulp Pretreatment.....	26
3.3 Ozonation Procedure.....	27
3.4 Analysis.....	28
3.4.1 Kappa Number Determination .....	29
3.5 Parameter Testing .....	31
3.5.1 Moisture Loss.....	31

3.5.2 Bed Height .....	32
3.5.3 Fibre Saturation Point .....	33
<b>Chapter 4 Effect of Pulp Type on the Rate of Delignification and Cellulose Degradation during Ozone Bleaching .....</b>	<b>34</b>
4.1 Introduction .....	34
4.2 Experimental .....	36
4.3 Results and Discussion .....	37
4.3.1 Effect of Consistency .....	40
4.3.2 Effect of Pulp Type .....	42
4.3.3 Effect of Pre-Bleaching Treatment .....	49
4.4 Conclusions .....	53
<b>Chapter 5 Effect of Fibre Properties on the Rates of Delignification and Cellulose Degradation.....</b>	<b>55</b>
5.1 Introduction .....	55
5.2 Theory .....	56
5.2.1 Generalized Expression for $\frac{\Delta K}{K_o}$ and $\frac{1}{DP_i} - \frac{1}{DP_o}$ .....	56
5.2.2 Determination of $w_o$ and $(\Delta K)_{Lumen}$ .....	59
5.3 Simplified predictive approach .....	61
5.4 Tortuosity and ECCSA .....	63
5.5 Generalized curves of delignification and cellulose degradation .....	66
5.6 Selectivity.....	70
5.7 Conclusions.....	70
<b>Chapter 6 General Conclusion .....</b>	<b>72</b>
6.1 Conclusions.....	72
6.2 Recommendations.....	72
6.3 Future Work.....	74
<b>Appendix A Cell Wall Thicknesses and Cell Diameter Distribution .....</b>	<b>76</b>
<b>Appendix B Pulp and Paper Terminology.....</b>	<b>80</b>
<b>References .....</b>	<b>82</b>

## LIST OF TABLES

<b>Table 3.1</b>	<b>Relationship between kappa number and %ISO Brightness measurements</b>	<b>30</b>
<b>Table 3.2</b>	<b>Fibre saturation point of each pulp type</b>	<b>33</b>
<b>Table 4.1</b>	<b>Properties of pulps studied</b>	<b>36</b>
<b>Table 4.2</b>	<b>Relationship between fibre saturation point and maximum rates</b>	<b>51</b>
<b>Table 5.1</b>	<b>Determination of the extent of delignification at optimum ozone delignification</b>	<b>61</b>
<b>Table 5.2</b>	<b>Gandek Constant as determined at the fibre saturation point</b>	<b>63</b>



## LIST OF FIGURES

<b>Figure 2.1</b>	Flowsheet for medium-consistency ozone bleaching system (Ahlstrom-Kamyr Inc.) [8]	5
<b>Figure 2.2</b>	Flowsheet for high consistency ozone bleaching system (Union Camp Corp.) [8]	6
<b>Figure 2.3</b>	Layout of the Union Camp Mill in Franklin, VA. [10]	7
<b>Figure 2.4</b>	TEM Micrographs of transverse sections of $\text{KMnO}_4$ stained Hemlock kraft pulp ozonated at $10^\circ\text{C}$ , pH of 2 for different lengths of time and extracted with 2% NaOH for 1.5 hours at $80^\circ\text{C}$ [14]	8
<b>Figure 2.5</b>	Shrinking core model of a fibre wall, showing the ozone concentration, lignin distribution and cellulose molecular weight distribution as a function of position [4]	9
<b>Figure 2.6</b>	Development of delignification with ozonation time [5]	11
<b>Figure 2.7</b>	Ozonolysis reaction with lignin [17]	14
<b>Figure 2.8</b>	Reaction of ozone with lignin, one electron reduction, and radical formation [17]	15
<b>Figure 2.9</b>	An electron micrograph of a thin section of a beaten kraft fibre after solvent exchange from water to an epoxy resin embedding reagent [20]	16
<b>Figure 2.10</b>	An electron micrograph of a thin section of a beaten kraft fibre after solvent exchange from water to an epoxy resin embedding reagent [21]	17
<b>Figure 2.11</b>	Optical micrograph of a transverse section of a delignified pine tracheid after extensive swelling in cuprammonium hydroxide and staining with congo-red [23]	18
<b>Figure 2.12</b>	Cell wall after a slight swelling in dilute cupraethylene diamine [22]	19
<b>Figure 2.13</b>	Schematic shrinking behaviour of the fibre wall cross section at different pulp consistencies [5]	19

- A- Pulp consistency below 40%, coated with an external liquid layer
- B- Pulp consistency at fibre saturation point
- C- Pulp consistency above the fibre saturation point
- D- Fully dry

<b>Figure 3.1</b>	Differential plug flow reactor	25
<b>Figure 3.2</b>	Schematic flow diagram for the experimental set-up	26
<b>Figure 3.3</b>	Relationship between ISO Brightness and Kappa Number	31
<b>Figure 3.4</b>	Effect of pulp mass on the extent of lignin removal and cellulose chain scission	32
<b>Figure 4.1</b>	Location of the ozone-lignin reaction front in pulp fibres during pulp ozonation. Darker inner core represents unreacted lignin. The light central core represents the lumen.	34
<b>Figure 4.2</b>	Development of delignification of cottonwood	37
<b>Figure 4.3</b>	Development of cellulose chain scission of cottonwood	38
<b>Figure 4.4</b>	Location of the ozone-lignin reaction front in pulp fibres during pulp ozonation. Darker inner core represents unreacted lignin. The light central core represents the lumen.	39
<b>Figure 4.5</b>	Effect of consistency on the rate of delignification of cottonwood	41
<b>Figure 4.6</b>	Effect of consistency on the rate of cellulose degradation of cottonwood	41
<b>Figure 4.7</b>	Lignin-carbohydrate selectivity of ozone in cottonwood pulp	42
<b>Figure 4.8</b>	The effect of softwood versus hardwood on the rate of delignification.	44
<b>Figure 4.9</b>	Softwood and hardwood pulps are indistinguishable from one another with respect to the rate of delignification	44

<b>Figure 4.10</b>	Representative guaiacyl and syringyl components of lignin	45
<b>Figure 4.11</b>	Softwood and hardwood cellulose degradation	46
<b>Figure 4.12</b>	A comparison of the typical shrinking core model behaviour of cottonwood with that of southern hardwood ( $K_0=6$ )	47
<b>Figure 4.13</b>	Ozone is more selective in hardwood pulps than in softwood pulps	48
<b>Figure 4.14</b>	Effect of pre-treatment on the rate of delignification. O versus OP pre-bleached pulp	50
<b>Figure 4.15</b>	Pre-treatment with peroxide accelerates the rate of cellulose chain scission during ozone bleaching	50
<b>Figure 4.16</b>	Effect of pulp consistency on delignification	52
<b>Figure 4.17</b>	Effect of pulp consistency on cellulose degradation	52
<b>Figure 4.18</b>	The lignin-carbohydrate selectivity of ozone for all pulp types studied.	53
<b>Figure 5.1</b>	Determination of $(\Delta K)_{\text{Lumen}}$ by integration of the cumulative fibre wall width distribution of cottonwood	60
<b>Figure 5.2</b>	Effective capillary cross-sectional area (ECCSA)	64
<b>Figure 5.3</b>	Tortuosity, $\lambda$ of the fibres	65
<b>Figure 5.4</b>	Generalized curve of delignification	67
<b>Figure 5.5</b>	Generalized curve of cellulose degradation	69
<b>Figure 5.6</b>	Generalized lignin-carbohydrate selectivity	71

## **NOMENCLATURE**

<b>a.d.t</b>	-	<b>Air dried ton</b>
<b>BOD</b>	-	<b>Biological oxygen demand</b>
<b>c</b>	-	<b>Pulp consistency (%)</b>
<b>c<sub>o</sub></b>	-	<b>Saturated ozone concentration in the liquid (kmol/m<sup>3</sup>)</b>
<b>COD</b>	-	<b>Chemical oxygen demand</b>
<b>D</b>	-	<b>Chlorine dioxide bleaching stage</b>
<b>D<sub>e</sub></b>	-	<b>Effective diffusion coefficient of dissolved ozone in swollen fibre wall(m<sup>2</sup>/s)</b>
<b>D<sub>m</sub></b>	-	<b>Molecular diffusion coefficient of ozone in a swollen fibre wall (m<sup>2</sup>/s)</b>
<b>DP</b>	-	<b>Average degree of polymerization of the cellulose chains</b>
<b>DP<sub>o</sub></b>	-	<b>Degree of polymerization of cellulose before ozonation</b>
<b>DP<sub>t</sub></b>	-	<b>Degree of polymerization of cellulose at an ozonation time (t)</b>
<b>DTPA</b>	-	<b>Diethylenetriaminepentaacetic acid</b>
<b>E</b>	-	<b>Caustic extraction stage</b>
<b>ECCSA-</b>	-	<b>Effective capillary cross sectional area, dimensionless</b>
<b>f<sub>1</sub>, f<sub>2</sub></b>	-	<b>Proportionality constants</b>
<b>FR</b>	-	<b>Final regime of ozone delignification</b>
<b>FSP</b>	-	<b>Fibre saturation point</b>
<b>g o.d.</b>	-	<b>grams oven dried</b>
<b>IR</b>	-	<b>Initial regime of ozone delignification</b>
<b>[L]<sub>o</sub></b>	-	<b>Lignin content in the reaction front (kg lignin/kg pulp)</b>
<b>[L]<sub>f</sub></b>	-	<b>Lignin content of unbleached pulp (kg lignin/kg pulp)</b>

- k, k<sub>l</sub>** - Proportionality constants
- k<sub>c</sub>** - Rate constant for cellulose degradation in the reaction front (DP·s<sup>-0.5</sup>·kPa<sup>-0.6</sup>)
- k'<sub>cf</sub>** - Rate constant for cellulose degradation in the reaction front (DP·s<sup>-0.5</sup>)
- k<sub>f</sub>** - Rate constant for delignification in the reaction front (kappa·s<sup>-0.5</sup>·kPa<sup>-0.5</sup>)
- k'<sub>lf</sub>** - Rate constant for delignification in the reaction front (kappa·s<sup>-0.5</sup>)
- K<sub>f</sub>** - Floor kappa value (kappa)
- K<sub>G</sub>** - Gandek Constant, (m·(kappa·kPa·s)<sup>-0.5</sup>)
- K<sub>o</sub>** - Kappa number of the unbleached pulp (kappa)
- K<sub>t</sub>** - Kappa number at a ozonation time, t (kappa)
- m** - Stoichiometry of fast lignin ozone reactions (kmol/kg lignin)
- O** - Oxygen delignified pulp
- OP** - Oxygen-peroxide delignified pulp
- [O<sub>3</sub>]\*** - Saturated ozone concentration in impregnation liquid (kmol/m<sup>3</sup>)
- [O<sub>3</sub>]<sub>f</sub>** - Average ozone concentration in the reaction front (kmol/m<sup>3</sup>)
- P<sub>o</sub>** - Ozone partial pressure in the bulk of the gas phase (kPa)
- t** - Ozonation time (s)
- t<sub>Lumen</sub>** - The time required for the reaction front to reach the lumen of a fibre (s)
- TEM** - Transmission electron microscopy
- TR** - Transition regime of ozone delignification
- w** - Fibre wall thickness (m)
- $\bar{w}$**  - The average width of the fibre wall (m)
- w<sub>co</sub>** - The fully collapsed fibre wall thickness (m)

- $w_f$  - Thickness of the thickest fibre wall (m)
- $w_o$  - Thinnest fibre wall thickness as determined at 10% of the total fibres (m)
- Z - Ozone bleaching stage
- $\Delta(1/DP)$ - Number of glucosidic bond cleavages in cellulose occurring during ozonation time, t.
- $\Delta K$  - Overall change in the kappa number during ozonation time t,  $K_o - K_t$  (kappa)
- $(\Delta K)_{Lumen}$  - Decrease in kappa number of the pulp at ozonation time of  $t_{lumen}$ , (kappa)
- $\alpha, \alpha'$  - Proportionality constants of the generalized rate of delignification
- $\beta, \beta'$  - Proportionality constants of the generalized rate of cellulose degradation
- $\delta$  - Position of the reaction front within the fibre wall (m)
- $\epsilon$  - Porosity of fibre wall ( $m^3$  void volume of fibre/ $m^3$  total volume of fibre)
- $\epsilon_{FSP}$  - Void fraction of the pulp at the FSP
- $\rho_l$  - Impregnating liquor density ( $kg/m^3$ )
- $\rho_w$  - Solid wood density ( $kg\ pulp/m^3$ )
- $\eta$  - Lignin-kappa number conversion factor
- $\lambda$  - Tortuosity, the dimensionless length of the diffusion path of a chemical in the direction of the fibre wall
- $(100-c)/c$  - Liquid holdup by the fibre wall ( $kg\ liquid/kg\ o.d.\ pulp$ )

## **CHAPTER 1 INTRODUCTION**

Due to increasing concern about the environmental impact of chlorinated organics formed during chlorine-based bleaching processes, ozone has received much attention as an alternate bleaching chemical. However the replacement of chlorine and chlorine dioxide with ozone for the production of fully bleached pulp is limited by its relatively poor lignin-carbohydrate selectivity [1]. Therefore industrial introduction of ozone pulp bleaching has been relatively slow [2].

Union Camp has developed a high consistency, ozone reactor [3]. Union Camp believes that for optimum sizing of the reactor for different wood pulp feeds, a fundamental understanding of the rate processes of delignification and cellulose degradation are required. The Limerick Pulp and Paper Centre at UNB has been studying the fundamentals of ozone bleaching for several years [1,2,4]. Most recently it has developed an experimental technique to measure the rates of delignification and cellulose degradation. A kinetic theory of delignification and cellulose degradation during ozone bleaching was first proposed by Griffin et al. [4], and was further developed by Zhang [5]. One of the variables still to be studied is the effect of pulp type as determined by wood species (softwood versus hardwood, thin-walled versus thick-walled fibres), kappa number, and treatment before ozone bleaching (unbleached, oxygen delignified (O and OP treated)). Since the rates of delignification and cellulose degradation are a strong function of pulp consistency, it is the objective of this study to measure the rates at different consistencies for the different pulp types.

## **1.1 OBJECTIVE AND STRATEGY**

The general objective is to study the effect of various fibre properties on the rate kinetics of delignification and cellulose degradation during high consistency ozone bleaching. The ultimate goal is the generation of predictive equations of the delignification and cellulose degradation rates for an untested pulp based on the physical and chemical data of the unbleached fibre. More specifically the objective is to determine the influence of the following parameters on the ozone bleaching kinetics:

- Wood species
- Ozonation pre-treatment
- Initial lignin content

The ozonation experiments were performed in a differential plug flow reactor. The following analyses were performed: CED viscosity, kappa number, and ISO brightness of the ozone treated and NaOH extracted pulp and fibre saturation point, kappa number and fibre cell wall thickness distribution of the untreated pulp. The rates of delignification and cellulose degradation were studied for consistencies between 26.2% and 78.2%. At each consistency samples of pulp were exposed to ozone for a predetermined period of time ranging from 5-120s. The ozonation temperature and ozone partial pressure were fixed at 10°C and 0.5 kPa respectively.

## **1.2 THESIS OUTLINE**

This thesis is concerned with the kinetics of ozone bleaching. The literature review in Chapter 2 provides the background required for this study. Included are an overview of the shrinking core model, the effect of consistency and fibre wall thickness



distribution, the chemistry of ozonation and the ozone bleaching technology of Union Camp. The experimental set-up and procedures are discussed in Chapter 3, while the effect of pulp type on the rates of delignification and cellulose degradation are investigated in Chapter 4.

Finally, the rates of delignification and cellulose degradation are predicted in Chapter 5 based on measurable pulp properties. Chapter 6 summarizes the contributions to knowledge and the future work arising from this study.

## **CHAPTER 2 LITERATURE REVIEW**

Especially during the 90's the pulp and paper industry has been driven by environmental concerns to find alternatives to the chlorine based bleaching sequences. There has been a move towards oxygen based bleaching chemicals, which could potentially yield strong, bright, environmentally friendly and affordable pulps [6].

Ozone has great potential as a bleaching agent, since it has the second highest electronegative oxidation potential, thereby making it one of the strongest oxidizing agents. When applied to unbleached pulp it was found to be an excellent delignification chemical. Ozone also has a low operating cost when compared with other non-chlorine bleaching agents, making it an attractive alternative from an economic standpoint [6]. Unfortunately it has also been found that the ozone charge must be limited to 1% on wood to avoid significant cellulose degradation and thereby excessive loss of strength in the resulting bleached pulp [7].

### **2.1 OZONE BLEACHING TECHNOLOGIES**

Commercially, both medium and high consistency ozone bleaching technologies are a reality. The medium consistency (MC) ozonation process involves the transfer of an acidified pulp-water suspension to a high-intensity mixer where it is mixed at high pressure with ozone gas. The gas is then separated from the pulp and the pulp is washed [8].

Prior to high consistency (HC) ozone treatment the pulp is acidified at a low consistency and thickened to 30-40% consistency. The pulp is then shredded and fluffed to increase the pulp surface area before it is fed into the gas-phase reactor where the pulp

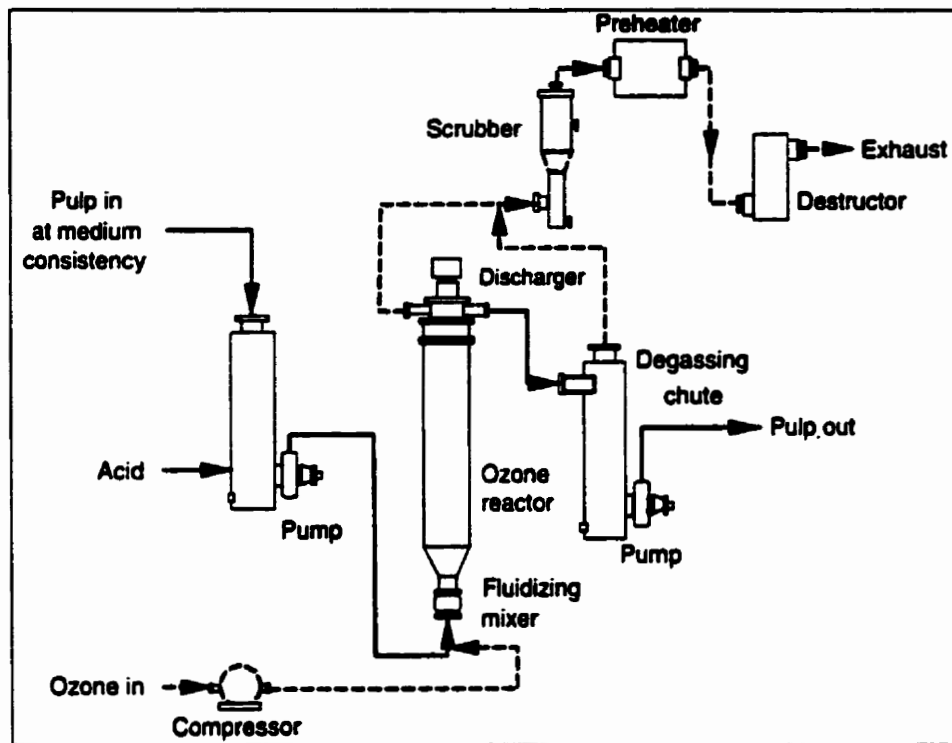


**Figure 2.1** Flow sheet for medium-consistency ozone bleaching system (Ahlstrom-Kamyr Inc.) [8]

fibres are dispersed in an ozone-oxygen gas phase. The pulp residence time in the reactor approaches plug flow to ensure uniform treatment of pulp with ozone. Schematics of the MC and HC ozone bleaching systems are represented in Figures 2.1 and 2.2 respectively [8].

The use of high consistency ozone bleaching allows for a high degree of delignification, efficient ozone consumption, efficient ozone utilization and complete filtrate recycle. Each of these goals is more difficult to meet under medium consistency bleaching conditions. High consistency bleaching can achieve a high brightness increase in a single, low pressure, stage [3], while multiple mixers and a high ozone pressure are required for MC ozone bleaching.

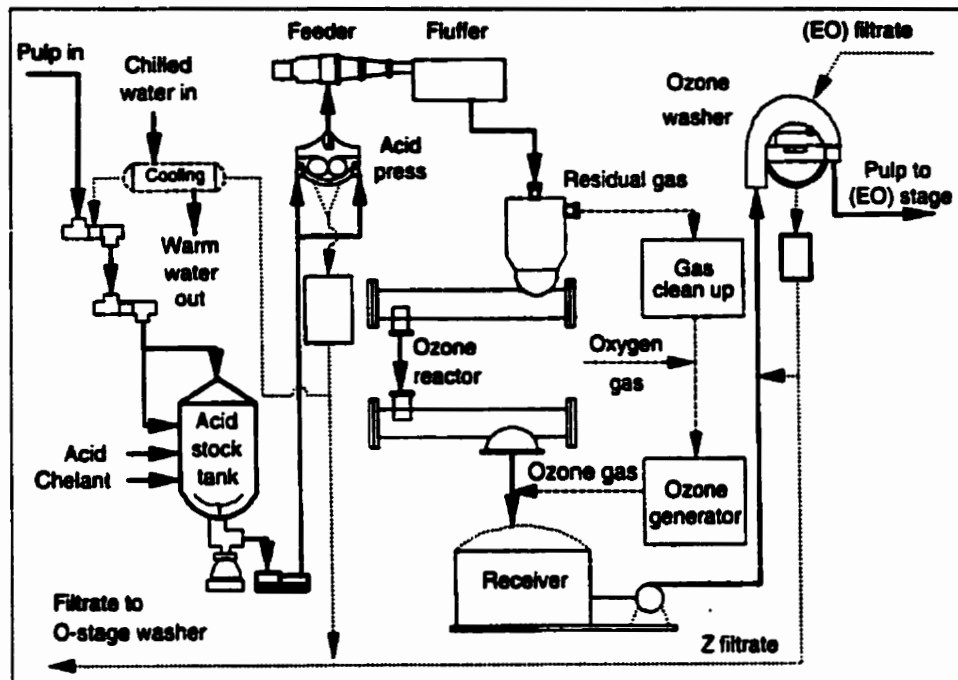


**Fig. 2.2** Flowsheet for high consistency ozone bleaching system (Union Camp Corp.) [8]

In terms of ozone bleaching, producing bleached pulps that are strong, bright and environmentally friendly is affected by the rate and uniformity with which ozone reacts with the pulp [9].

## 2.2 COMMERCIAL HC OZONE BLEACHING

The Union Camp Mill in Franklin, VA has designed a HC ozone based bleaching sequence capable of handling 1000 a.d.t of conventional batch cooked, screened pine brown stock (see Figure 2.3). The driving force behind implementing the high consistency OZ(EO)D sequence was the need to lower water usage, effluent color and BOD levels at the mill [10].

After the oxygen stage (O), the pulp is passed through two washing presses before being split into two parallel ozone stages (Z). Each ozone stage has a capacity of 500 a.d.t per day, with the reactors being operated below 1 psig. The pulp is passed through a

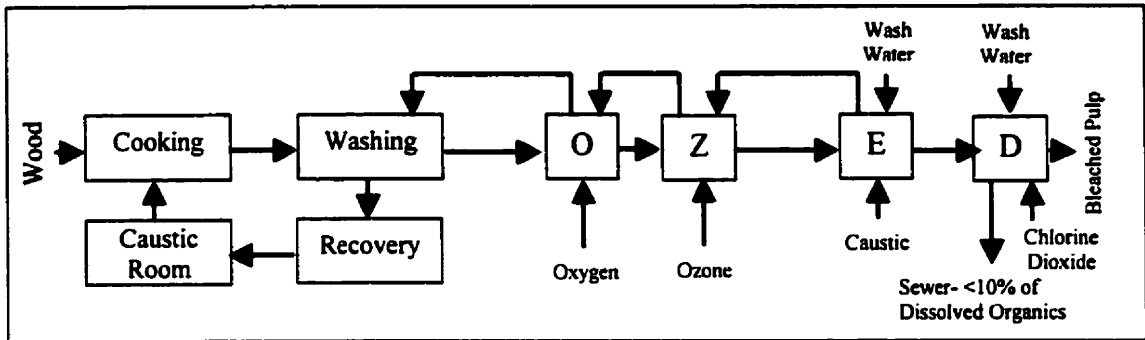


**Figure 2.3** Layout of the Union Camp Mill in Franklin, VA [10].

displacement chest to bring the stock consistency to upwards of 35%. The high consistency pulp is then fluffed in a high consistency fluffer and conveyed via a pressure lock into the ozone reactor. The ozone enters at the pulp discharge and flows countercurrent to a separation device at the pulp feed [11]. It is applied at 12.5-15 lbs/a.d.t of unbleached stock, depending on the brightness of the oxygen stage outlet. There is a 95% consumption of ozone, which indicates effective gas-pulp mixing in the ozone reactor. A 15 point increase in ISO brightness can be realized in the ozone stage with minimal drop in viscosity (14.1 cP entering and 10.3 cP leaving the reactor) [11].

The OZ(EO)D sequence ensures obtaining pulps with a final brightness of 83%. It reduces the chloroorganic compound emissions to the 0.03-0.04 kg/t level on pulp, BOD levels to 1-2 kg O<sub>2</sub>/t, COD levels to 2-6 O<sub>2</sub>/t, and color to 0.5-1.5 kg pt/t (the lower value refers to hardwood pulps, the higher ones, to softwood pulp). In comparison with the traditional CEDED sequence it means an 88% reduction of BOD, a 91% reduction of COD, 85% reduction in chloroorganic compounds and a reduction in the effluent volume by 86% [12].

### 2.3 MODELLING OF OZONE BLEACHING KINETICS

It is well known that ozone reacts quickly with lignin, therefore mass transfer resistances must be considered when studying the kinetics of ozone bleaching. Three potential steps have been identified which could limit the rate of delignification of pulp fibres during high consistency ozone treatment [13]. They are,

1. Transfer of ozone from the bulk gas phase in the pores to the surface of the fibre wall.
2. Dissolution of ozone in the liquid phase of the fibre wall followed by diffusion through the pores in the fibre wall to reactive sites.
3. Chemical reaction with lignin.

Diffusion of ozone through the liquid filled pores inside the fibre wall has been determined to be the controlling step for the rate of ozone delignification [5,6,10,13,14]. In this situation, the kinetics of delignification can be described by the rate of movement of a sharp ozone-lignin reaction front moving through the fibre wall from the fibre surface to its lumen [4].

Zhang[5] made transmission electron micrographs of  $\text{KMnO}_4$ -stained ozonated

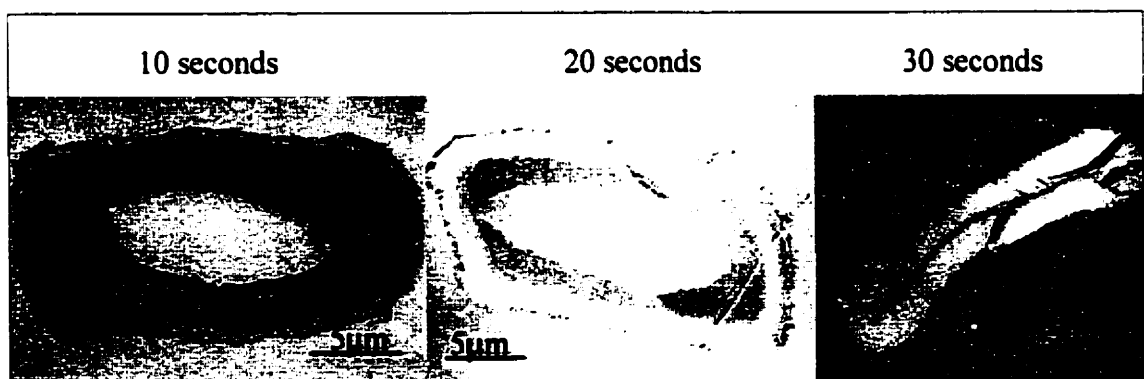


**Figure 2.4** TEM micrographs of transverse sections of  $\text{KMnO}_4$  stained Hemlock Kraft pulp ozonated at  $10^\circ\text{C}$ , pH of 2 for different lengths of time and extracted with 2% NaOH for 1.5 hours at  $80^\circ\text{C}$  [14]

pulp fibres, to show the existence of the sharp ozone-lignin reaction front. Cross sections of  $\text{KMnO}_4$  stained fibre walls clearly shows a sharp separation between a lighter reacted region and darker region inside the fibre wall [14] (see Figure 2.4). The lighter region is indicative of a low lignin content while the darker region shows the original, unbleached lignin content. As ozonation time increases the sharp reaction front moves progressively towards the lumen of the fibre, while the rate of movement of the front is limited by the diffusion of ozone through the pores. The presence of the visible reaction front is proof of the ozone diffusion rate being the rate controlling step during pulp ozonation.

The physical model describing the movement of the reaction front is referred to as the shrinking core model with reacted layer diffusion control [15]. The rate of conversion of the solid reactant, lignin, is limited by diffusion of the chemical, ozone, to the reaction

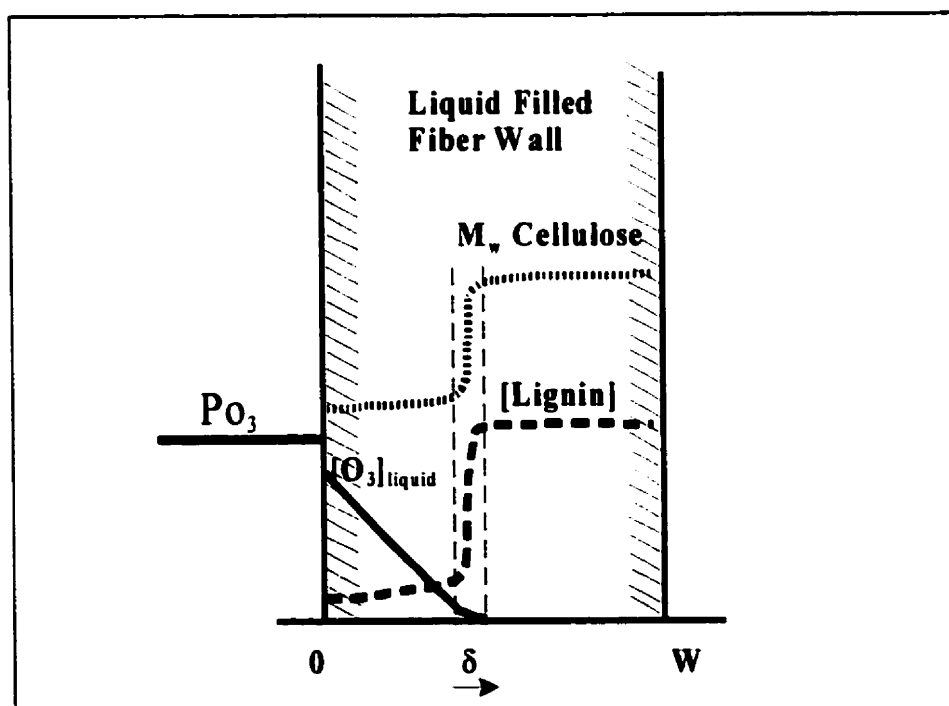


**Figure 2.5** Shrinking core model of a fibre wall, showing the ozone concentration, lignin distribution and cellulose molecular weight distribution as a function of position [4].

site. Figure 2.5 represents a schematic picture of the shrinking core model for a fibre wall. The fast delignification reactions occur at the lignin-ozone front, and are completed in the region between the external fibre surface and the reaction front. Ozone in the bulk gas surrounding the pulp fibres diffuses into the water-filled pores of the fibre wall. The dissolved ozone then diffuses through the pores in the reacted part of the fibre wall towards the front where it reacts with the lignin. Because of the fast reaction of ozone with lignin, a reaction front is established which forms a sharp division between the unreacted and reacted lignin regions. As the ozonation time increases, the reaction front,  $\delta$ , moves inward through the fibre from the external fibre surface toward the lumen. The rate of ozone diffusion through the liquid filled pores in the fibre wall governs the rate of movement of the sharp ozone-lignin reaction front, which in turn dictates the rate of delignification [5]. At the reaction front, the concentration of ozone is very low because of its fast reaction with lignin. Cellulose does not react with ozone at a rate comparable to that of the ozone-lignin reaction. However, at the reaction front, cellulose is simultaneously attacked and degraded by the hydroxyl radicals generated during the ozone-lignin reaction. Therefore, a reaction front between the cellulose that has and has not been degraded is established and moves parallel with the lignin-ozone reaction front through the fibre wall.

Using the shrinking core model, equations have been developed for the reaction kinetics of delignification and cellulose degradation of pulp fibres during ozone bleaching. Griffin et al. [4], have derived an equation which describes the position of the reaction front within the fibre wall as



$$\delta = 1.5 \left( \frac{[O_3]^* D_e t}{m[L]_0 \rho_w (1-\epsilon) \epsilon} \right)^{1/2} \quad (2.1)$$

Where  $[O_3]^*$  is the saturated ozone concentration ( $\text{kmol/m}^3$ ) in the impregnation liquid,  $D_e$  is the effective diffusion coefficient ( $\text{m}^2/\text{s}$ ) of ozone in the fibre wall,  $t$  is the ozonation time (s),  $m$  is the stoichiometry ( $\text{kmol/kg}$  lignin) of the fast lignin-ozone reactions,  $[L]_0$  is the lignin content ( $\text{kg}$  lignin/ $\text{kg}$  pulp) of unbleached pulp,  $\epsilon$  is the porosity ( $\text{m}^3$  void volume in fibre/  $\text{m}^3$  total volume in fibre) of the fibre wall, and  $\rho_w$  is the solid wood density ( $\text{kg}$  pulp/ $\text{m}^3$ ). Equation 2.1 suggests that the rate of delignification

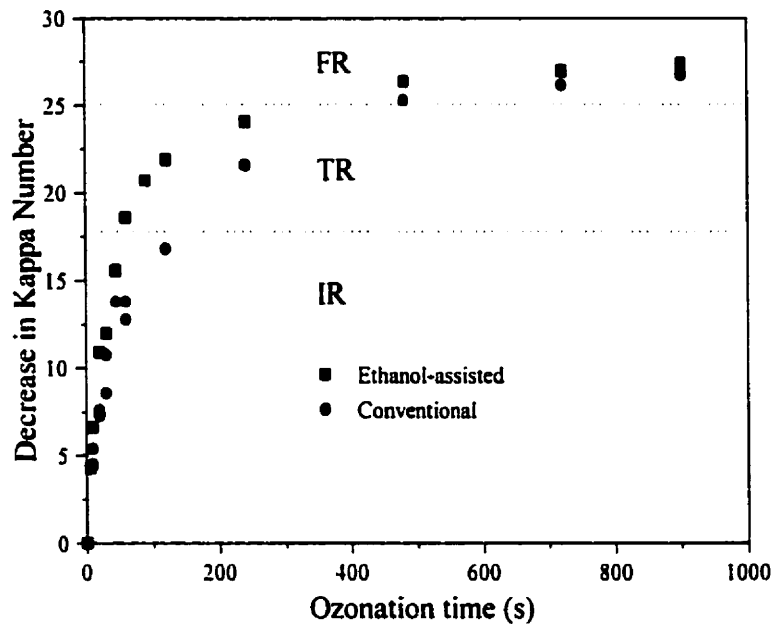


**Figure 2.6** Development of delignification with ozonation time [5].

is proportional to the square root of the ozonation time.

Zhang [5] has found that three regions of delignification can be identified during ozone bleaching. Zhang termed the initial portion of delignification the initial regime (IR), the asymptotic plateau, the final regime (FR) and the region of the delignification

curve connecting the two, the transition regime (TR), Figure 2.6. Zhang[5] determined that the shrinking core model describes the initial rate of delignification very well, with the rate of delignification being proportional to the square root of ozonation time. However in the transition regime deviation from the linear relationship occurs. Finally the rate slows down dramatically, and the extent of delignification reaches an asymptotic plateau.

Based on the shrinking core model, Zhang [16] developed equations to describe the rates of delignification and cellulose degradation for the initial regime. If it is assumed that the lignin content is uniformly distributed throughout the unbleached fibre wall then

$$\frac{K_o - K_t}{(\Delta K)_{\text{Lumen}}} = \frac{\Delta K}{(\Delta K)_{\text{Lumen}}} = \frac{\delta}{w} \quad (2.2)$$

where  $\Delta K$  is the decrease in kappa number of the pulp from the  $K_o$ , initial kappa number to  $K_t$  the pulp kappa number at time  $t$ , and  $(\Delta K)_{\text{Lumen}}$  is the decrease in kappa number when the lignin reaction front has reached the lumen for the fibres with the thinnest fibre wall thickness ( $w$ ).

Since  $w = w_{co}(1 - \varepsilon)$  and  $(\Delta K) = \eta[L]_o$ , where  $\eta$  is a lignin-kappa number conversion factor, and  $w_{co}$  is the fully collapsed fibre wall thickness (m), combining the above equations with the equation for the position of the ozone-lignin reaction front, the extent of delignification is expressed as

$$\Delta K = k_1 \left( \frac{[O_3] D_c [L]_o (1 - \varepsilon) \cdot t}{mw_{co}^2 \rho_w \varepsilon} \right)^{0.5} = k_{if} (P_o \cdot t)^{0.5} = k'_{if} t^{0.5} \quad (2.3)$$

where  $P_o$  is the ozone partial pressure in the bulk of the gas phase (kPa) and  $k_{if}$  and  $k'_{if}$  are the rate constants of delignification ( $kappa^{0.5}/(kPa \cdot s)^{0.5}$  and  $kappa/(s)^{0.5}$  respectively).

By assuming that a fixed fraction of the ozone-lignin reaction leads to radical generation (i.e. a constant yield), and that a small fixed fraction of these radicals results in cellulose chain scissions, it can be derived [16] that

$$\Delta\left(\frac{1}{DP}\right) = \left(\frac{[O_3]_f [L]_f c_o D_e t}{m L_o \rho_w (1-\epsilon)\epsilon}\right)^{0.5} = k_c P_o^{0.6} t^{0.5} = k'_c t^{1/2} \quad (2.4)$$

where DP is the average degree of polymerization of the cellulose chains,  $\Delta(1/DP)$  is the number of glucosidic bond cleavages in cellulose occurring during ozonation time,  $t$  and  $k_c$  and  $k'_c$  are the rate constants of cellulose degradation at the ozone-lignin reaction front ( $DP^{-1} \cdot kPa^{-0.6} \cdot s^{-0.5}$  and  $DP^{-1} \cdot s^{-0.5}$  respectively).

Zhang has confirmed experimentally that the rate of delignification during ozone bleaching of kraft fibres is proportional to the square root of ozone partial pressure, the initial lignin content, and the ozonation time. He also confirmed that the initial lignin content has no effect on the rate of cellulose degradation [5].

The rate of cellulose degradation as measured by the increase in number of cellulose chain scissions, behaves similarly to the rate of delignification during the initial regime of ozonation. However, in the final regime the rate of cellulose degradation is caused by ozone direct attack and is proportional to the ozonation time. In contrast, the rate of delignification reaches a plateau in the final regime. For this reason the optimal ozonation time has been found to be at the end of the initial regime, when the rate of delignification slows down with ozonation time faster than the rate of cellulose

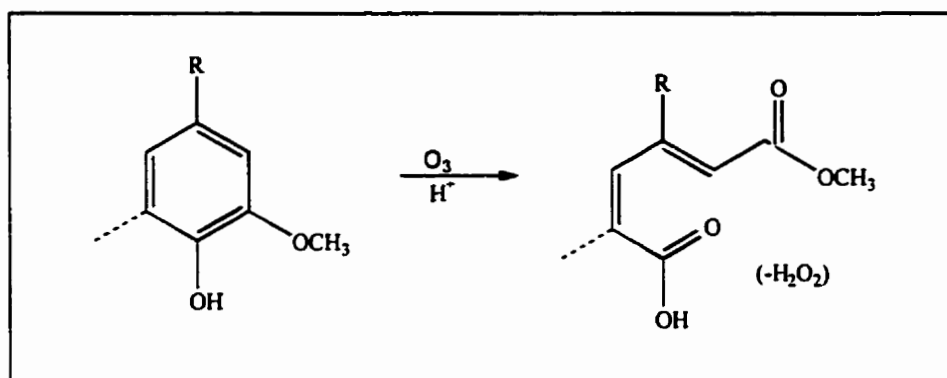


**Figure 2.7** Ozonolysis reaction with lignin [17]

degradation. Therefore, the end of the initial regime represents the optimum point of delignification and beyond this point the lignin-cellulose selectivity decreases.

Gandek [9] used the shrinking core model to predict the delignification rate at the fibre saturation point for a given pulp. Based on Zhang's delignification equation (2.3) he confirmed that the rate of delignification is proportional to the square root of the initial kappa number  $K_0$ , divided by its collapsed fibre wall thickness,  $w$ . This agreement supports the validity of the shrinking core model as the basis for describing and predicting the intrinsic rates of delignification during the initial regime of ozonation.

## 2.4 CHEMISTRY OF DELIGNIFICATION AND CELLULOSE DEGRADATION

Ozone reacts with lignin and most organic substrates by ozonolysis. As a delignifying agent, ozone is very selective in that it will react with lignin model compounds extremely quickly, while exhibiting relatively little reactivity toward cellulose model compounds. The ionic cyclo-addition to and cleavage of activated aromatic and olefinic bonds (Figure 2.7) has been reported as the main pathway for ozone to react with lignin model compounds [17].

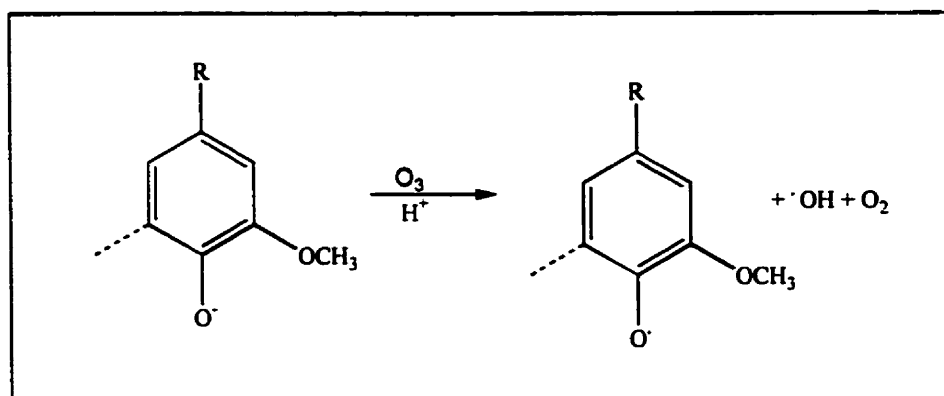


**Figure 2.8** Reaction of ozone with lignin, one electron reduction, and radical formation [17]

Easily oxidized organic substrates such as phenolates give up an electron to the ozone molecule. This leads directly to the formation of hydroxyl radicals, which unlike ozone are very unselective and will attack both lignin and carbohydrates, Figure 2.8.

The yield of radicals produced as a direct result of the reaction of ozone with phenolate type structures varies depending on the exact nature of the compound. The reaction of ozone with vanillin produces a 12% yield of radicals, syringaldehyde has a yield of 28%. Hardwood contains an approximate lignin makeup of 50/50 syringyl and guaiacyl structures, of which syringaldehyde and vanillin are representatives respectively. Softwood contains mainly guaiacyl lignin structures. Therefore it is speculated that a higher selectivity of ozone for lignin over carbohydrates would be more easily attained for softwoods [18].

Cellulose is degraded by both direct attack of ozone and by attack of secondary radical species. Zhang [19] found that in conventional ozone bleaching of Hemlock kraft pulp (kappa of 31) the vast majority of the cellulose degradation occurs by radical attack at the reaction front. About 7.5% of cellulose degradation between the outer wall of the fibre and the ozone-lignin reaction front is also the attack of radical species, which only

accounts for a few percent to the total cellulose chain scissions during pulp ozonation. Finally, the direct attack of ozone only accounts for about 25% of the cellulose degradation in the reacted region.

## 2.5 FIBRE WALL STRUCTURE

Kerr and Goring [20] suggested a detailed lamellar model for the cell wall of a softwood fibre. Figure 2.9 illustrates the lamellar layer of crystalline cellulose covered by amorphous lignin and hemicellulose after delignification during cooling the majority of the lignin and a significant fraction of the hemicellulose is removed. This creates an extensive porous network, which provides a pathway for the movement of reagents into, and for lignin, out of the cell wall during bleaching [22].

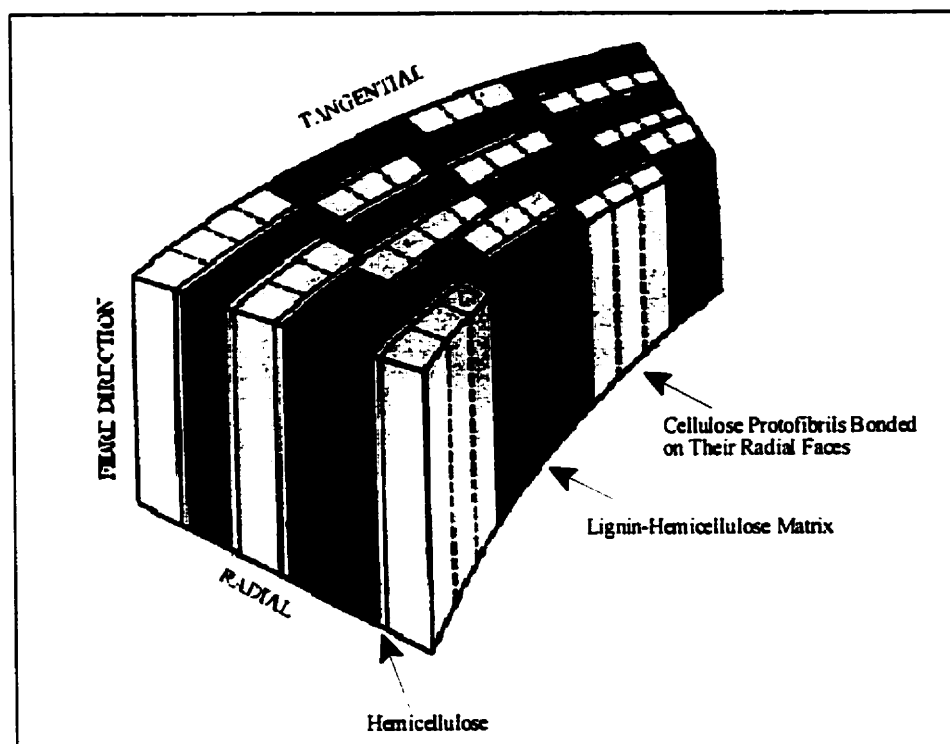


**Figure 2.9** Detailed Lamellar model of the ultrastructure of the fibre wall [20]



**Figure 2.10** An electron micrograph of a thin section of a beaten kraft fibre after solvent exchange from water to an epoxy resin embedding reagent [21]

According to Scallan [22] the cell wall of a softwood fibre consists of a concentric arrangement of lamellae. When totally dry, all the hydroxyl groups of the carbohydrate structures bond to one another, creating a tightly packed arrangement of microfibrils (Figure 2.10). As water penetrates into the cell wall of chemical fibres, the lamellae begin to swell. Figure 2.11 represents the fully swollen state of the fibre wall. In a partially swollen state, water preferentially enters the tangentially oriented planes between the microfibrils causing partial swelling. To a lesser extent, water also penetrates and breaks the radially oriented bonds, creating a microfibrillar structure that has more of a homeycomb appearance (Figure 2.12). As the amount of water absorbed into the fibre wall increases to the point of saturation, the degree of separation between the microfibrils increases, beyond this point the cell is fully swollen and its structure remains unchanged [22]. Pictorially this is represented by A and B in Figure 2.13.

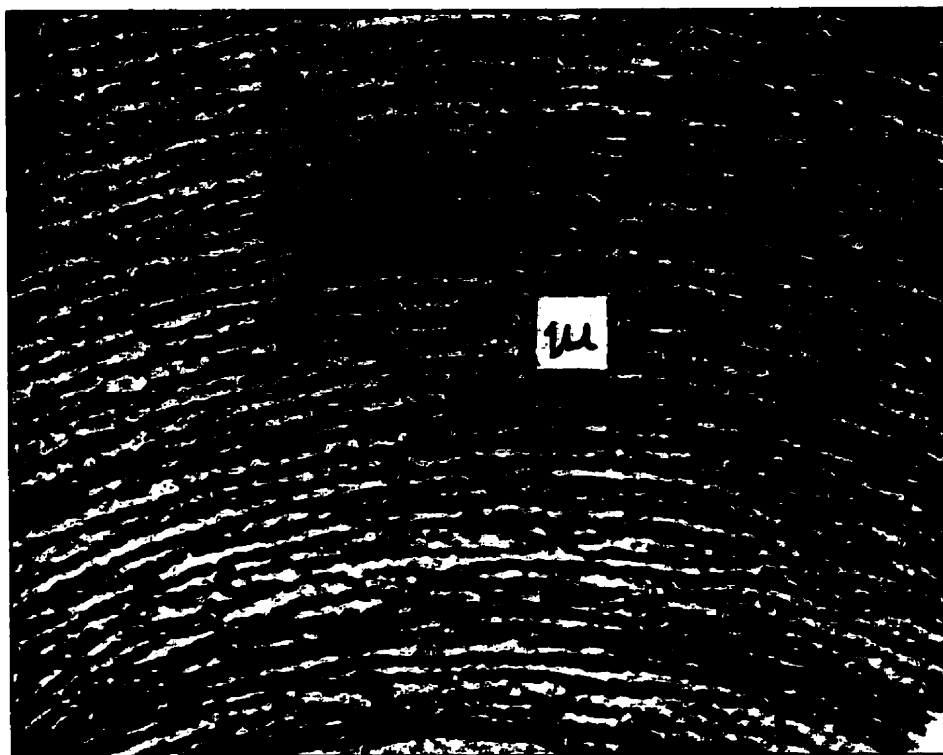


**Figure 2.11** Optical Micrograph of a transverse section of a delignified pine tracheid after extensive swelling in cuprammonium hydroxide and staining with congo-red [23]

Two parameters are used to quantify the effective diffusional transport through a fibre wall, ● the Effective Capillary Cross Sectional Area, ECCSA, and ● the tortuosity,  $\lambda$ . The ECCSA describes the non-dimensional diffusional transport as the ratio of the effective diffusion to the molecular diffusion. The ECCSA of wood is expected to be different than that of pulp since the diffusion through the fibre wall and the lumen of many cells must be considered as opposed to diffusion through a single fibre wall respectively [24]. For a fully cooked kraft pulp fibre the pore structure of the fibre wall is greatly enlarged due to the removal of most of the lignin and hemicellulose during the pulping process [5].



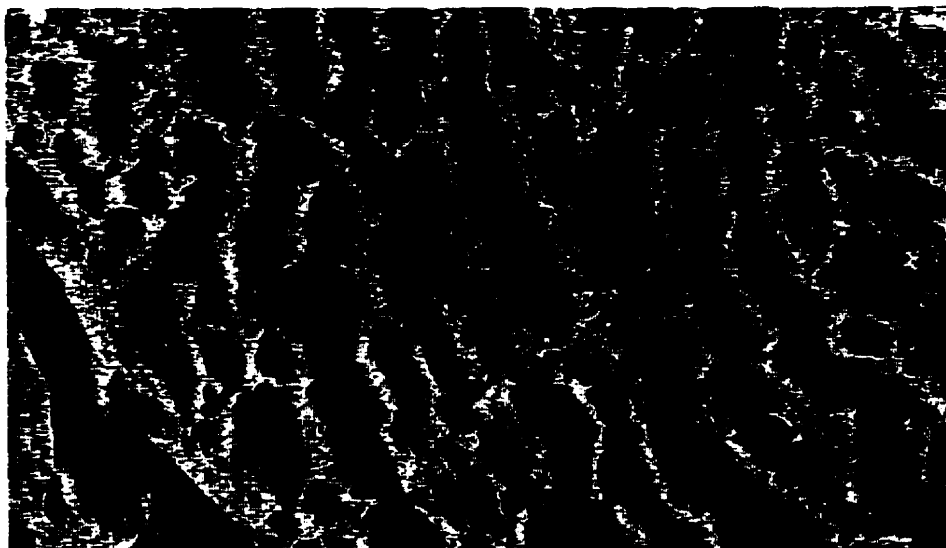


**Figure 2.12** Cell wall after a slight swelling in dilute cupraethylene diamine [22]

Tortuosity,  $\lambda$ , is the dimensionless length of the diffusion path of a chemical through a porous material. It is defined as  $\lambda = \frac{D_m \varepsilon}{D_c}$ , providing the relationship between

ECCSA and tortuosity as  $\lambda = \varepsilon / \text{ECCSA}$ .

Zhang [18] calculated the ECCSA of Hemlock kraft pulp ( $K_o=31$ ) and oxygen-

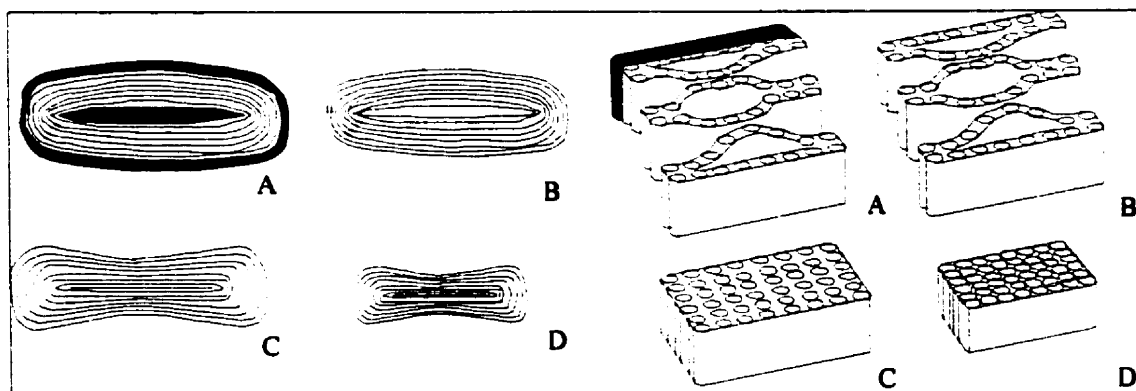


**Figure 2.13** Schematic shrinking behaviour of the fibre wall cross section at different pulp consistencies [5]  
 A- Pulp consistency below 40%, coated with an external liquid layer  
 B- Pulp consistency at fibre saturation point  
 C- Pulp consistency above the fibre saturation point  
 D- Fully dry

Hemlock kraft pulp ( $K_o=18.5$ ). The ECCSA and  $\lambda$  were calculated for consistencies between 21-70%, the tortuosity was constant at a value of 7 up to 55% consistency, while the ECCSA decrease from its maximum value of 0.09 at the fibre saturation point of 42% for the Hemlock kraft pulp. The two parameters were independent of initial lignin content and the ozone partial pressure in the bulk gas surrounding the fibre [5].

## 2.6 FIBRE WIDTH DISTRIBUTION

According to the shrinking core model the rate of delignification during high consistency ozone bleaching is determined by the diffusion of ozone through the fibre wall. During the initial regime of ozonation the ozone-lignin reaction front has not reached the lumen for the majority of fibres, i.e. the shrinking core model is valid for essentially all the fibres of different cell wall thicknesses. As thinner fibres become fully penetrated in the transition regime, the overall delignification reaction rate decreases. The rate diminishes further and finally becomes zero as the thickest fibre becomes totally penetrated. At this point the rate of delignification reaches its asymptotic plateau.

The rate of cellulose degradation does not decrease in a similar fashion as the reaction front penetrates fibres of ever increasing cell wall thickness. The reason for this is that the direct attack of cellulose by ozone increases after full delignification because the ozone concentration is now at the saturation value uniform through the fibre wall. During the final regime the rate of cellulose degradation is proportional to the ozonation time.

Bennington [13] took the fibre width distribution for the pulp sample into account when modeling the entire range of delignification and cellulose degradation for the

Hemlock and oxygen-Hemlock kraft pulp of Zhang [5]. The model required values for the shrinking core velocity constant for lignin removal ( $k'$ ), the floor kappa number ( $k^f$ ), the floor level of DP for cellulose degradation from radical attack ( $DP^f$ ), the reaction rate constant for radical attack ( $k_{CR}$ ) and direct attack ( $k_{CD}$ ) of ozone on cellulose, the ozone consumption per unit drop in kappa ( $dO_3/dt$ ), as well as the initial kappa and degree of cellulose polymerization, temperature and pH of reaction. Equation 2.5 was solved for small increments of time, and then Equation 2.6 is integrated numerically for these small time steps, and K and DP for the entire pulp sample was calculated as the front progressively moves through the fibre.

$$\delta = \sqrt{\frac{2D_e Co_3 t}{mL_o \rho_b}} = k' P_o^{0.5} t^{0.5} \quad (2.5)$$

$$\frac{d\delta}{dt} = \frac{D_e Co_3}{mL_o \rho_b \delta} = \frac{k P_o}{\delta} \quad (2.6)$$

The model was successful in accurately predicting the entire delignification and cellulose degradation of the Hemlock pulps.

## 2.7 EFFECT OF CONSISTENCY

The effect of consistency on the rates of delignification and cellulose degradation has been reported by many. Osawa and Schuerch [25] found that the rate of ozonation is highest when the fibre is saturated but not surrounded by water. Secrist and Singh [26] found that the rate reaches a maximum at ~40%. Liebergott et al. [7] investigated the effect of consistency between 25% and 60%. They found that an increase in consistency from 25% to 53% was accompanied by a corresponding decrease in kappa number.

Beyond 53% consistency the effect was no longer apparent. Also as the consistency increased, less ozone was required per unit kappa number drop.

Zhang [24] studied the rates of delignification and cellulose degradation at pulp consistencies of 23% to 77%. The maximum rates of delignification and cellulose degradation were observed at a consistency of about 50% which is higher than the fibre saturation point of 42-44%.

At consistencies below the fibre saturation point, a higher pulp consistency means a thinner water layer on the outside surface of the fibres for the ozone to diffuse through before further diffusion and reaction in the fibre wall. As the consistency increases, the external water layer becomes thinner offering less mass transfer resistance to the ozone.

At consistencies above the fibre saturation point, there is no external liquid layer, and an increase in pulp consistency leads to shrinkage of the intra-lamellar between the fibrillar layers. This shortened path for the diffusional transport of ozone leads to an increase in the rate of ozone diffusion and therefore delignification.

As the consistency is increased further above the fibre saturation point, less and less water is associated with the fibre and as shrinkage occurs the path for ozone diffusion through the fibre wall becomes more hindered because of pore closure. At this point the rate of delignification starts to decrease with increasing consistency. In other words the decrease in rate about 50% consistency can be explained by the dominance of pore closure over the shrinking of the fibre wall and the rate decreases continually with increasing consistency [5].

Zhang derived that the effect of consistency on rate constants of delignification and cellulose degradation, as well as the definition of tortuosity can be described as [5].

$$k'_{lf} = 1.5 \left( \frac{[O_3] \cdot D_m \cdot \rho_l}{m [L]_0 w_o^2 \rho_w^2} \right)^{0.5} \left( \frac{c \times \text{ECCSA}}{100 - c} \right)^{0.5} (\Delta K)_{\text{Lumen}} \quad (2.7)$$

$$k'_{cf} = 1.5 \left( \frac{[O_3]^{(1-2x)} \cdot D_m \cdot \rho_l}{m \cdot w_o^2 \cdot \rho_w^2} \right)^{0.5} \left( \frac{c \times \text{ECCSA}}{100 - c} \right)^{0.5} \quad (2.8)$$

$$\lambda = \left( \text{ECCSA} \times \left( 1 + \frac{\rho_l}{\rho_w} \left[ \frac{c}{100 - c} \right] \right) \right)^{-1} \quad (2.9)$$

where  $[O_3]$  is the saturated ozone concentration ( $\text{kmol/m}^3$ ) in the liquid,  $D_m$  is the molecular diffusivity of ozone in the liquid phase ( $\text{m}^2/\text{s}$ ),  $m$  is the stoichiometry ( $\text{kmol/kg}$  lignin) of the fast lignin ozone reactions,  $[L]_0$  is the lignin content ( $\text{kg}$  lignin/ $\text{kg}$  pulp) of unbleached pulp,  $w_{co}$  is the fully collapsed fibre wall thickness ( $\text{m}$ ),  $\rho_l$  is the liquid density ( $\text{kg/m}^3$ ),  $\rho_w$  is the wood density ( $\text{kg/m}^3$ ), and  $c$  is the pulp consistency (%). Zhang found  $(\Delta K)_{\text{Lumen}}$  to be a constant fraction ( $\sim 0.6$ ) of  $K_o$  [5].

## **CHAPTER 3 EXPERIMENTAL**

All experiments were performed in a differential plug flow reactor kept isothermally at 10°C. The moisture inside the pulp was adjusted to a pH of 2 and the ozone partial pressure was maintained at 0.5 kPa, with a total air flow of 4 L/min.

The pulp samples studied were supplied by Union Camp, and each pulp sample was stored in a refrigerator throughout the study. The pulp types studied were:

1. Kraft-O Southern Pine (K<sub>o</sub> ~ 14)
2. Kraft-OP Southern Pine (K<sub>o</sub> ~ 15)
3. Kraft-O Southern Hardwood (K<sub>o</sub> ~ 9)
4. Kraft-O Southern Hardwood (K<sub>o</sub> ~ 6)
5. Kraft-O juvenile Cottonwood (K<sub>o</sub> ~ 13)

In order to determine the intrinsic kinetics of ozone bleaching it is important that the ozone supply rate be kept at such a high level as to ensure that the ozone concentration around individual fibres is essentially the same and constant. The intrinsic kinetics of ozone bleaching can then be determined by measuring the change in lignin content and pulp viscosity as a function of the ozonation time.

### **3.1 EXPERIMENTAL SET-UP**

Experiments were performed in a plug flow differential reactor (Figure 3.1). The reactor used was a 6 cm (inside diameter), 350 ml Pyrex® wash bottle with an extra coarse porous glass distributor. Gas was introduced to the pulp via the distributor at the base of the reactor. The well-fluffed nature of the pulp fibres and the small amount of

pulp, along with the high gas flow rate, ensured that all of the fibres were exposed to approximately the same inlet gas concentration [27].

An electric timer and a three way solenoid valve were used to accurately control the ozonation time over a range of 5 to 120 s. The ozone was generated by passing a constant flow of dry air through a PCL Model 1 ozone generator. The air flow rate into the ozone generator, and hence the production rate of the ozone, was kept constant at

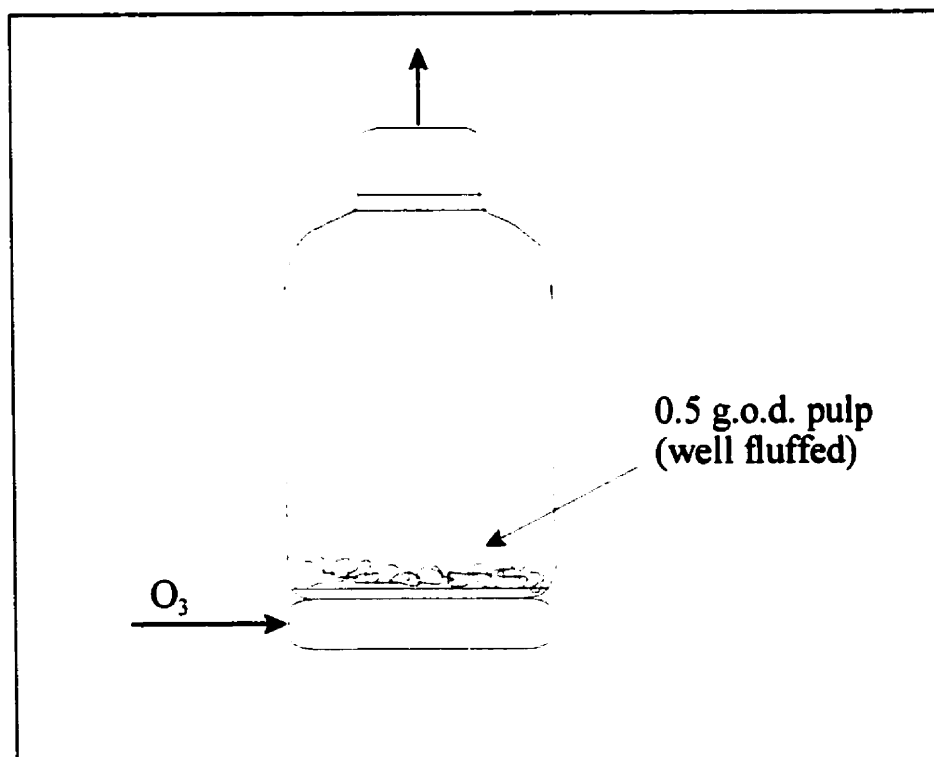


**Figure 3.1** Differential plug flow reactor.

2L/min. Before entering the differential reactor, the ozone containing air stream was diluted to 4 L/min with a 2 L/min stream of compressed air. Between ozonation tests, the 2 L/min ozone stream was redirected to an acidified sodium thiosulfate tank for neutralization. To purge, or remove ozone from the reactor, 4 L/min compressed air was sent during 120 seconds through the reactor. The gas flow rates were held constant using

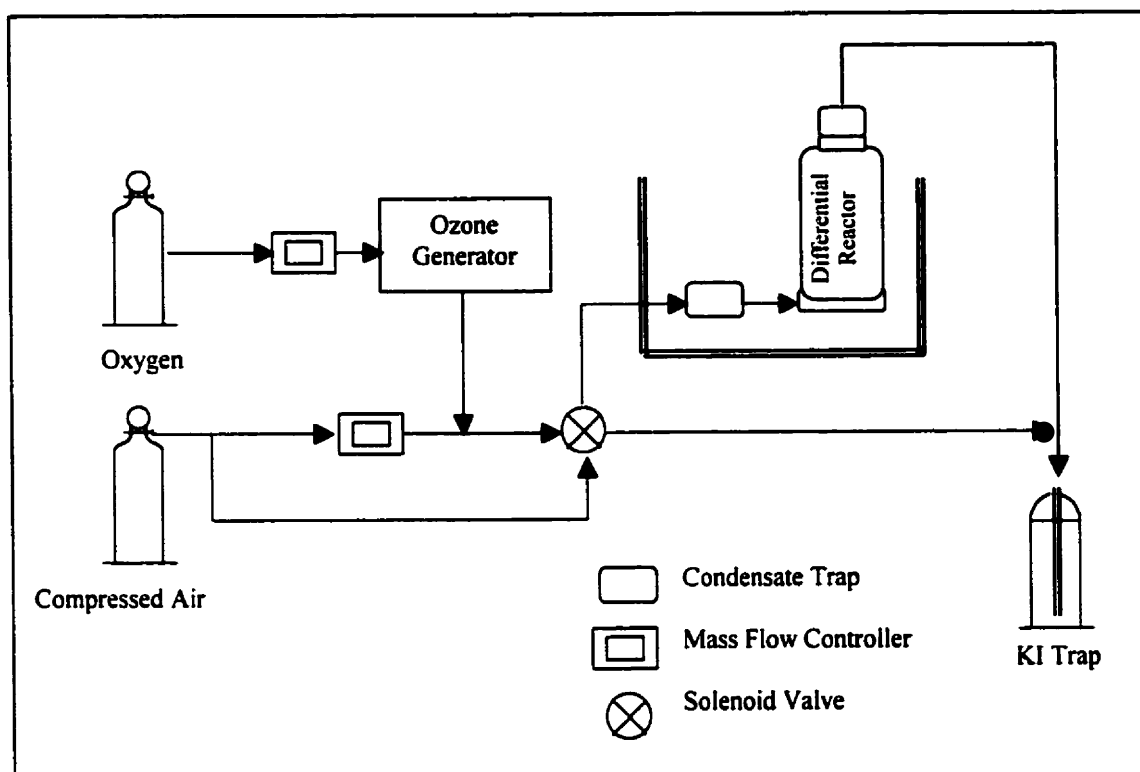


**Figure 3.2** Schematic flow diagram for the experimental set-up

mass flow controllers. A schematic flow diagram for the experimental set-up is shown in Figure 3.2.

### 3.2 PULP PRETREATMENT

Typically, 50 g o.d. dried pulp was brought to a consistency of 1% in distilled, deionized water and acidified using  $\text{H}_2\text{SO}_4$  to a pH of 2. After 30 minutes the pulp was washed three times and again diluted. It was treated at 20°C with DTPA (0.5% charge on pulp) at a consistency of 1% for 30 minutes at a pH of 5, washed and stored in the refrigerator for future use. The acid and DTPA treatments were performed to remove metal ions. The residual Cu, Fe, and Mn contents were shown to be 0.4, 6.0, 0.3 ppm (on o.d. pulp) respectively, after this treatment [14]. These values are low enough as to not affect ozone decomposition.



### **3.3 OZONATION PROCEDURE**

For each experiment, approximately 10 g o.d. pulp was impregnated for 10 minutes by kneading the pulp with 750 ml acidified water at a pH of 2. The pulp was then filtered and brought to a desired consistency by pressing and centrifugation. After being treated in a fluffer contactor operated at 3450 rpm for 10 seconds, the pulp was transferred into a closed plastic bag for moisture equilibration. After two hours, the pulp was re-luffed and a pulp sample was taken to determine its moisture content. For experiments that required high consistencies, the 10 g o.d. pulp was placed in the differential reactor and dry air was forced through it before it was transferred into the plastic bag.

For each ozonation experiment, 0.5 g o.d. pulp (unless otherwise specified) was carefully packed into the differential reactor at an even bed height. The reactor was then submerged in a constant temperature bath of 10°C and left for ten minutes as the pulp bed reached temperature equilibrium.

The inlet and outlet of the reactor were covered during the 10 minutes prior to ozonation to avoid any fluctuations in moisture content. Ozonation time began when 4 L/min of ozone was introduced into the reactor and stopped by the electric solenoid valve once the desired ozonation time was reached. The reactor was immediately purged with dry air to remove any residual ozone from the reactor.

The pulp was then washed with deionized water and transferred to a plastic bag. At a consistency of 1% it was extracted in a caustic solution of pH 12 and 80°C for 1.5 hours. After extraction, the pulp was again washed with deionized water and air dried for further analysis.

Prior to each series of ozone experiments performed at a given consistency, the ozone concentration was tested and its partial pressure adjusted to 0.5 kPa. To do this, the 4 L/hr of ozone containing gas was charged for 30 seconds to the reactor and then sent to an absorption vessel containing 1% potassium iodide in water, and finally all gas was purged from the system by compressed air. The KI solution in the vessel was then acidified and titrated against sodium thiosulfate to determine the ozone concentration. The ozone partial pressure was set by adjusting the amount of current applied to the oxygen stream of the ozone generator, and the ozone concentration was measured again until the correct ozone pressure was achieved.

For each pulp type the intrinsic kinetics of bleaching were determined at various pulp consistencies. The determination of the intrinsic kinetics at a particular consistency involved the ozonation of eight to ten 0.5 g o.d. pulp samples, each having a set ozonation time between 0-120 s. Duplicate experiments were conducted for each time interval.

### **3.4 ANALYSIS**

The delignification and cellulose degradation rates for each pulp type were evaluated at various pulp consistencies ranging from 30-70%. At each consistency a number of well fluffed pulp samples were exposed to ozone gas for a controlled length of time. To determine the extent of lignin removal or cellulose degradation resulting from ozone treatment it is necessary to compare the measured kappa and viscosity values for the ozonated pulp samples with unbleached pulp samples. Therefore, at each consistency a pair of pulp samples was prepared following the same procedure as for the ozonated

pulp samples. The control samples were not exposed to ozone treatment but were extracted in caustic.

Due to the small quantity of pulp used for each experiment, handsheets were prepared using a modification of a Revised TAPPI Standard Method (T 218 om-91)[28]. In order to maintain the handsheet thickness required for brightness testing, the Büchner funnel of nominal 150 mm inside diameter was replaced by one of 25 mm inside diameter. All other parameters and testing procedures remained as stated in the standard testing method.

The viscosity and lignin content were measured according to modified viscosity and kappa tests (see also Section 3.4.1) described by Zhang [5]. Fibre saturation point determination was measured in accordance with the centrifugal method described by Scallan [29]. Brightness testing was performed according to the TAPPI standard method (T 525 om-92) [28].

The cell wall thickness and fibre diameter distribution for each sample was determined by Econotech Services Ltd.(See Appendix A).

#### **3.4.1 Kappa Number Determination**

Usual practice for determining lignin content of a pulp sample is to perform the TAPPI Standard Method [28] for kappa number determination (T236 cm-85) on 1-35 g of pulp. In the present study the experiments were performed with relatively small samples of pulp (maximum of 0.5 g o.d.) for each experiment. Therefore the modified kappa test, as developed by Zhang [5], was used to determine the lignin content. This test utilizes much smaller samples of pulp, while still giving results within 6% of the TAPPI

Standard test, which is well within experimental error of that test. The modified test requires 0.02-0.15 g o.d. pulp to be dispersed in 10 ml of acidified permanganate solution. This test is appropriate for kappa numbers ranging from 31 to 2.

Most of the pulps used in this work had a low initial kappa number ranging from 6 to 15. Ozone reacts quickly and efficiently with lignin, sometimes reducing the kappa number to values below a kappa number of two. Below a kappa number of two the modified kappa test the mass of pulp becomes too large to be dispersed in the available solution. Therefore an accurate measurement is not possible at the lowest kappa numbers.

Brightness is a measure of the reflectance of blue light by a handsheet. As the reflectance increases so does the whiteness of the sheet. Since lignin is the chemical species that primarily imparts colour to the pulp, brightness was used as a measure of the amount of lignin present in the pulp for kappa numbers below about three. Brightness and kappa tests were performed on pulp samples of a given species with kappa numbers

**Table 3.1 Relationship between Kappa Number and %ISO Brightness measurements**

<b>Pulp Type (all kraft)</b>	<b>% ISO Brightness</b>	<b>R<sup>2</sup></b>
Cottonwood	$-1.77(\text{kappa}) + 71.6$	0.97
Southern Hardwood (K <sub>o</sub> =6)	$-2.53(\text{kappa}) + 78.7$	0.96
Southern Hardwood (K <sub>o</sub> =9)	$0.18(\text{kappa})^2 - 4.77(\text{kappa}) + 72.5$	0.96
OP Southern Pine	$0.11(\text{kappa})^2 - 3.91(\text{kappa}) + 67.5$	0.98

greater than about two. The relationship between ISO Brightness and kappa number for each pulp type is shown in Figure 3.3 with the correlation given in Table 3.1. In addition to measuring absorption of light by the lignin chromophores, brightness measurements account for the reflective index of the handsheet surface. Consequently the relationship between kappa number and ISO brightness is not constant for all pulp types. For the very low kappa numbers the ISO Brightness measurements were used to calculate kappa

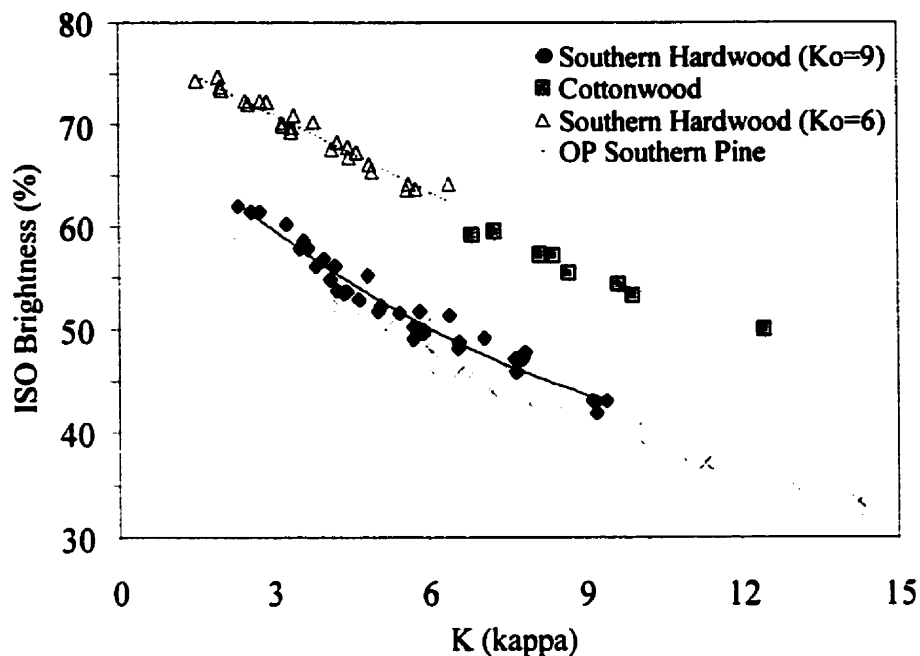


**Figure 3.3** Relationship between ISO Brightness and kappa number

number by extrapolating the appropriate relationship between kappa number and ISO brightness for each pulp type.

### 3.5 PARAMETER TESTING

#### 3.5.1 Moisture Loss

The exact moisture content of the pulp sample during ozonation is required therefore it was determined whether or not the application of 4L/min gas flow for the duration of the ozonation and purge stages changed the moisture content of the pulp.

The consistency of the pulp during ozonation was determined by testing the moisture content of the bulk pulp sample at the beginning and end of each consistency experiment. A 0.5 g o.d. pulp sample was prepared as if it were to be ozonated. After the ten minutes of temperature conditioning in the constant temperature bath, the pulp sample was removed from the reactor and immediately the consistency of the sample was

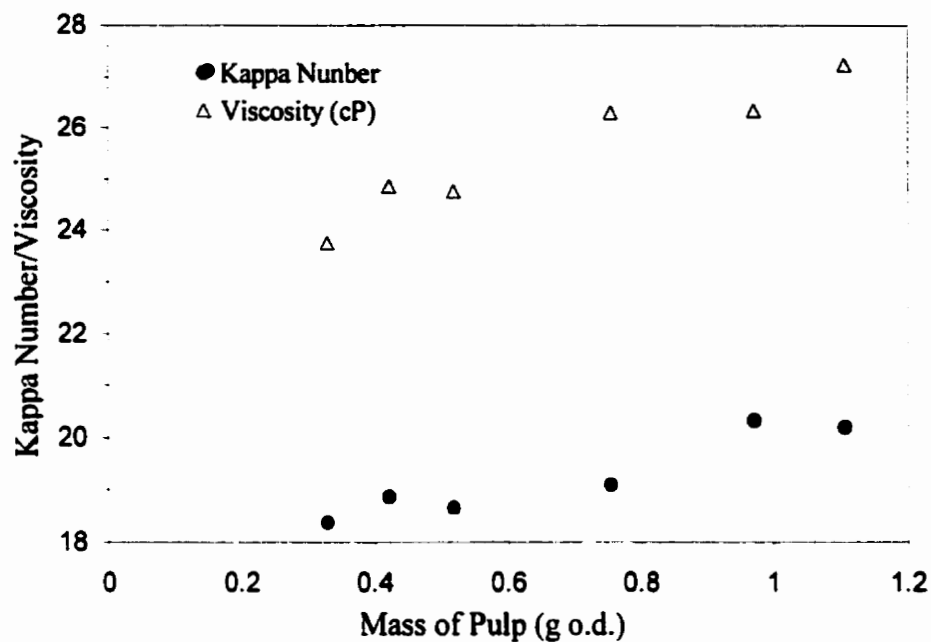


**Figure 3.4** Effect of pulp mass on the extent of lignin removal and cellulose chain scission.

determined. Then the consistency of another 0.5 g o.d. sample was measured after 60 seconds of compressed air purging in addition to the temperature conditioning period. On comparing the consistencies, each was found to be 46.75%, with or without the 60 second purge, showing that at the present conditions the moisture content of the pulp does not change due to the exposure to dry air.

### 3.5.2 Bed Height

It was important during this experimental regime to insure that each fibre was equally exposed to the same ozone concentration. In other words, the ozone supply must be high enough that the fibres in the higher region of the bed are exposed to the same ozone concentration as those in the lower part of the bed. Therefore, standard experiment was performed on pulp beds of different mass. They were packed into the differential reactor and treated with ozone for 15 seconds. The pulp was then extracted with caustic, dried and tested for loss in kappa number and drop in CED viscosity. According to the

results, shown in Figure 3.4, the extent of delignification and cellulose degradation decreases slightly with increasing pulp mass (greater bed height). In order to minimize this error all experiments were performed using 0.5 g o.d. pulp.

### 3.5.3 Fibre Saturation Point

The fibre saturation point was measured for each of the pulp types tested. The fibre saturation points were determined according to the procedure outlined by Scallan [29] and are summarized in Table 3.2

**Table 3.2** Fibre saturation point of each pulp type

<b>Pulp Type</b>	<b>FSP %</b>
Kraft-Hemlock	42
Kraft-O Southern Pine ( $K_o \sim 14$ )	41
Kraft-OP Southern Pine ( $K_o \sim 15$ )	40
Kraft-O Southern Hardwood ( $K_o \sim 9$ )	41
Kraft-O Southern Hardwood ( $K_o \sim 6$ )	41
Kraft-O juvenile Cottonwood ( $K_o \sim 13.5$ )	37

## CHAPTER 4

### EFFECT OF PULP TYPE ON THE RATES OF DELIGNIFICATION AND CELLULOSE DEGRADATION DURING OZONE BLEACHING

#### 4.1 INTRODUCTION

Despite excellent delignification, the industrial introduction of ozone bleaching has been slow because of concern regarding excessive cellulose degradation, chemical cost and actual reactor performance. For optimum sizing of an ozone reactor for different pulp types, a fundamental understanding of the rate processes of delignification and cellulose degradation is needed. It has been shown [14] that the progress of delignification and cellulose degradation during ozone bleaching can be described by the movement of a lignin (and cellulose) degradation front through the fibre wall from the external fibre surface to the lumen (Figure 4.1). The rate of delignification is determined by diffusion of ozone through the reacted fibre wall region between the external surface and the ozone-lignin reaction front. The cellulose degradation takes place mostly inside the front by radical species generated by fast lignin-ozone reactions. Based on this

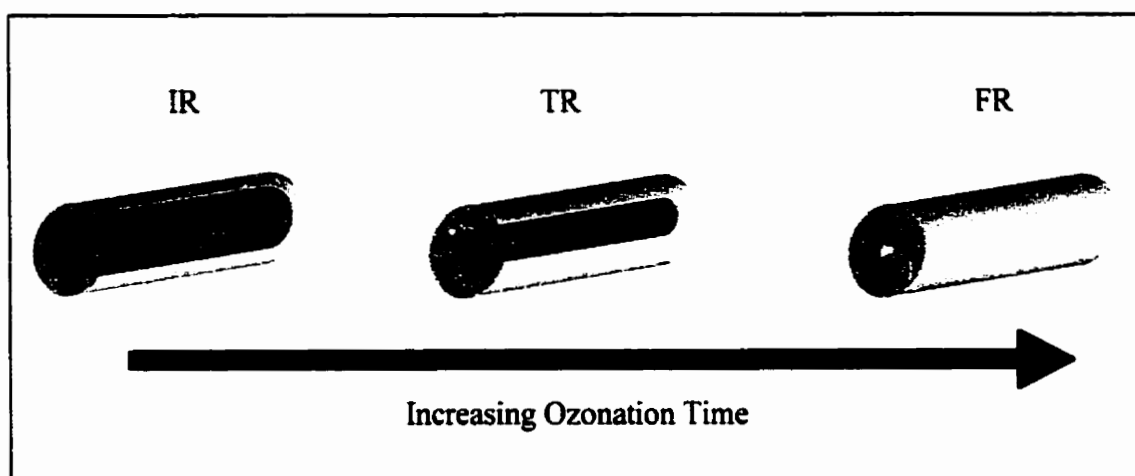


**Figure 4.1** Location of the ozone-lignin reaction front in pulp fibres during pulp ozonation. Darker inner core represents unreacted lignin. The light central core represents the lumen.



mechanism, a quantitative description of the effect of ozone partial pressure, temperature and kappa number on the ozonation kinetics was reported [16] for Hemlock kraft pulp.

The influence of pulp type on the rates of delignification and cellulose degradation during ozone bleaching has not been extensively reported in literature. Kamishima et al. [30] showed that hardwood kraft pulps brighten more easily than softwood pulps at the same ozone consumption, indicating a higher rate of delignification for hardwood pulps. Liebergott and van Lierop [7] found similar rates of delignification for unbleached hardwood and unbleached softwood pulps, although oxygen pre-bleached hardwood pulps showed a higher rate of delignification than softwood.

Similarly, the rate of cellulose degradation of unbleached and oxygen pre-bleached hardwood and softwood was found to be different. Liebergott and van Lierop [31] found that the viscosity of softwood pulp and hardwood pulp, was lower when bleached using ozone (ZDED) compared to traditionally (CEDED) bleached. It has also been shown by Liebergott and van Lierop [7] that the decrease in viscosity for hardwoods and softwoods was greater in unbleached pulps than in those that had been treated with oxygen prior to ozonation. Lindholm [32], on the other hand found that the viscosity drop in ozone bleached oxygen delignified pulps was greater than that observed for unbleached pulps. This suggests that further investigation into the ozonation kinetics of unbleached and oxygen pre-bleached pulps is necessary. Also, although hardwoods and softwoods have been evaluated against one another, the effect of species within both classes has not been investigated.

It is the objective of the present study to quantify the effect of pulp type as determined by wood species (softwood versus hardwood, thin-walled versus thick-walled

fibres), kappa number, and treatment before ozone bleaching (unbleached, oxygen delignified (O) and OP treated) on the ozonation kinetics. Since the rates of delignification and cellulose degradation are a strong function of pulp consistency [23], these rates have been measured at consistencies covering a range from about 30% to 70% for the different pulp types.

## 4.2 EXPERIMENTAL

The differential plug flow reactor developed and tested by Zhang [5] was used in the present study. The ozonation temperature and ozone partial pressure were fixed at 10°C and 0.5 kPa respectively. Each pulp type was treated at several different consistencies (varying from 30-70%) according to the procedure described in Chapter 3. At each consistency a 0.5 g o.d. sample of well fluffed, acidified pulp was exposed to ozone for a predetermined period of time ranging from 5-120s. After ozonation the pulp samples were extracted with caustic, washed and prepared as 2.5 cm diameter handsheets for the determination of lignin content and extent of cellulose degradation.

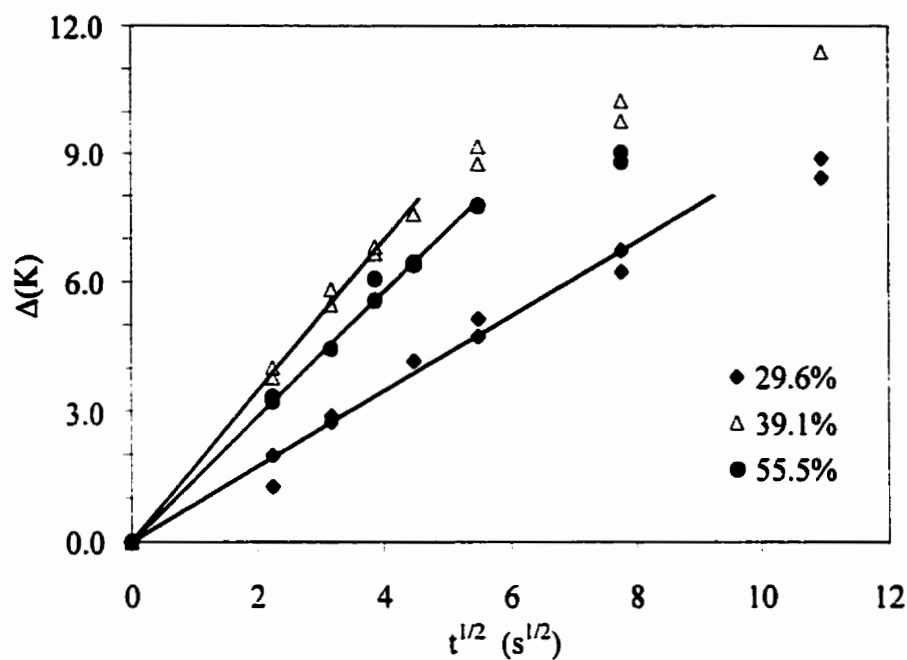
For illustration purposes the measurement procedure and interpretation of the data

Table 4.1 Properties of pulps studied

Pulp Type (all kraft)	Kappa Number	Pulp Viscosity (cP)	Average Fibre Wall Thickness ( $\mu\text{m}$ )	Fibre Saturation Point (%)
O Cottonwood	13	54	4.1	35
O Southern Hardwood	9	34	5.1	41
O Southern Hardwood	6	12	5.3	41
OP Southern Pine	14	24	5.7	40
O Southern Pine	15	24	5.7	41
Hemlock*	31	35	4.6	42
O Hemlock*	18.5	27	NR	NR

\* data from Zhang [5]

NR- not reported



**Figure 4.2** Development of delignification of cottonwood.

will be presented in detail for the experiments with cottonwood pulp. All the other pulp types were treated in the same manner as cottonwood. The properties of the pulps studied are listed in Table 4.1.

### 4.3 RESULTS AND DISCUSSION

The development of delignification and cellulose degradation during ozone bleaching of cottonwood at 29.6%, 39.1%, and 55.5% consistency is shown in Figure 4.2 and Figure 4.3 respectively. Two regimes of ozone delignification can be identified in Figure 4.2 (see literature review, page 11). The initial regime is characterized by a linear relationship between the decrease in kappa number and the square root of ozonation time. This behaviour is consistent with the shrinking core model kinetics described in Chapter 2. During the initial period the reaction front has moved some distance into the pulp fibre

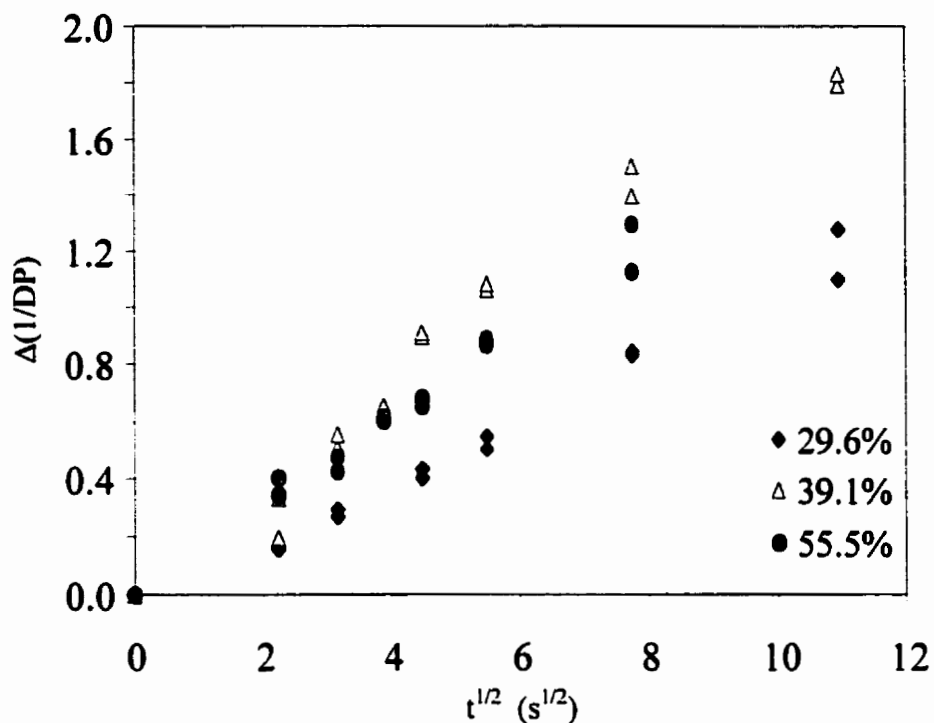


**Figure 4.3** Development of cellulose chain of cottonwood.

wall, but has not reached the lumen for any significant number of fibres. It is during this regime that the bulk of the delignification occurs. The ozone concentration is at the saturation value corresponding to the gas concentration at the external fibre wall surface. It then decreases linearly through the fibre wall to a concentration of zero at the reaction front. The fast ozone-lignin reactions and associated hydroxyl radical generation ensures that the rates of delignification and cellulose degradation are high during this period.

The onset of the transition regime in Figure 4.2 is characterized by the deviation from linearity of the relationship between decrease in kappa number and the square root of ozonation time. It occurs when the reaction front has reached the lumen for an increasing number of fibres (see Figure 4.4). During the final regime the reaction front has reached the lumen for the majority of pulp fibres. Thus the final regime is

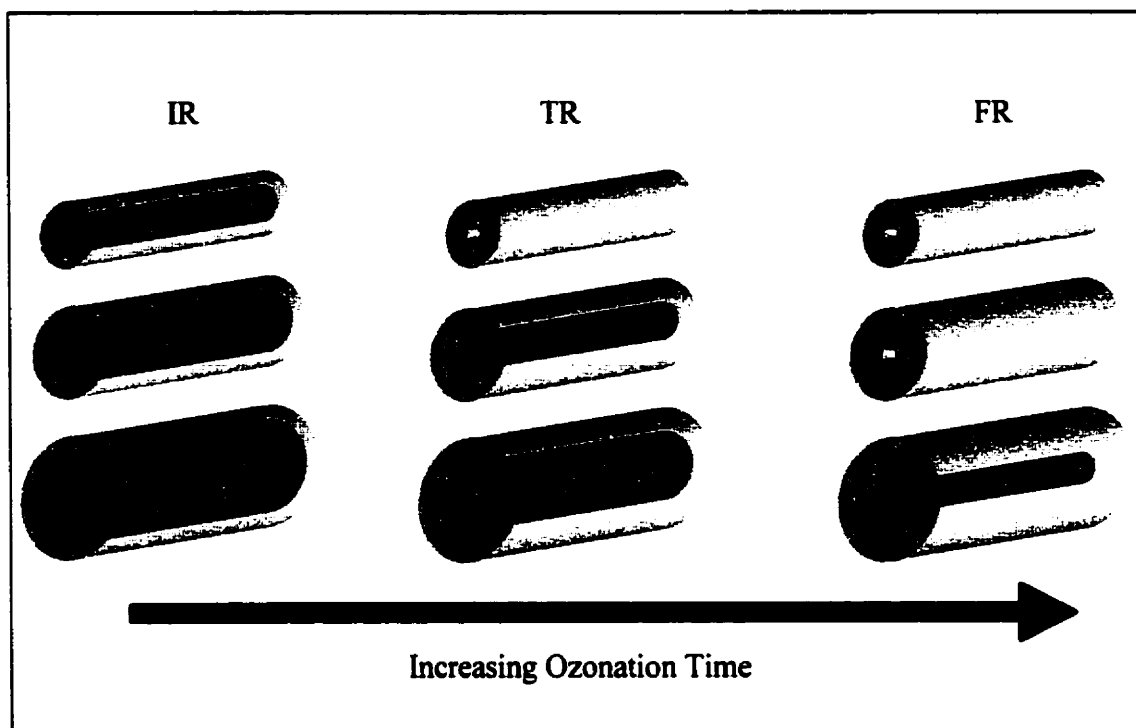


**Figure 4.4** Location of the ozone-lignin reaction front in pulp fibres of varying diameter. Darker inner core represents unreacted lignin. The light central core represents the lumen.

characterized by a minimal increase in delignification accompanied by an increase in cellulose degradation that is almost linear with respect to ozonation time. This regime is not reached in the present experiments shown in Figures 4.2 and 4.3.

From Figure 4.2 it is evident that for the present range of pulp consistencies, the end of the initial regime occurred as the kappa number of cottonwood ( $K_o=13$ ) was reduced by about eight units. This is a reduction of approximately 60%. The total change in kappa number up to the end of the initial regime will be called  $(\Delta K)_{\text{Lumen}}$ . Since the rate of cellulose degradation decreases less rapidly than the rate of delignification in the intermediate regime,  $(\Delta K)_{\text{Lumen}}$  represents the optimum lignin removal during ozone bleaching.

### 4.3.1 The Effect of Consistency

The rates of delignification and cellulose chain scission at different consistencies are determined as the slope of the straight lines representing the initial regime in Figures 4.2 and 4.3 respectively. The rate constant of delignification ( $k'_{lf}$ ) and that of cellulose chain scission ( $k'_{cf}$ ) for cottonwood pulp are shown as a function of consistency in Figures 4.5 and 4.6 respectively. It is apparent from these figures that the kinetics of ozonation strongly depend on pulp consistency. Both the rates of delignification and cellulose degradation display a maximum as a function of consistency. For the cottonwood pulp, the maximum occurs at a pulp consistency of about 40-45%, which is slightly above the fibre saturation point of cottonwood of 37%. The following explanation can be given for the existence of the maximum in the ozonation kinetics with consistency.

At consistencies below the fibre saturation point, the amount of water external to each pulp fibre becomes less with increasing consistency, and as a result the mass transfer resistance offered by this water layer also decreases. At the fibre saturation point there is no external water anymore, and all the fluid is contained within the fibre walls. As the consistency increases above the FSP the intra-lamellar between the fibrillar layers begins to shrink. Initially this shrinkage leads to a shortened path for the diffusional transport of ozone through the fibre and a corresponding increase in rate of delignification. At the same time the decrease in water associated with each of the pulp fibres leads to an ever decreasing effective capillary cross sectional area (ECCSA). A maximum rate of delignification and consequently cellulose degradation

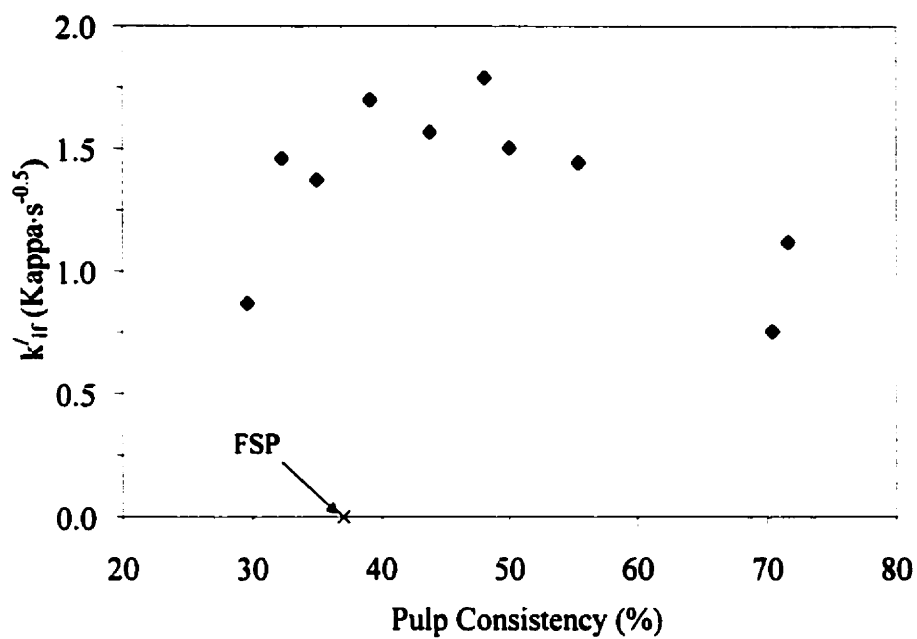


**Figure 4.5** The effect of consistency on the rate of delignification of cottonwood.

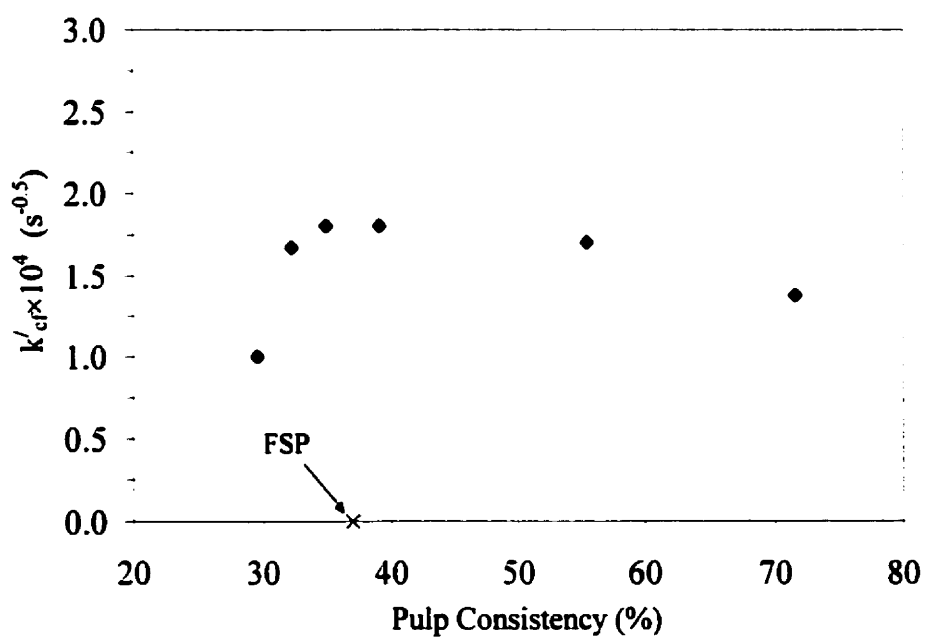


**Figure 4.6** The effect of consistency on the rate of cellulose degradation of cottonwood.

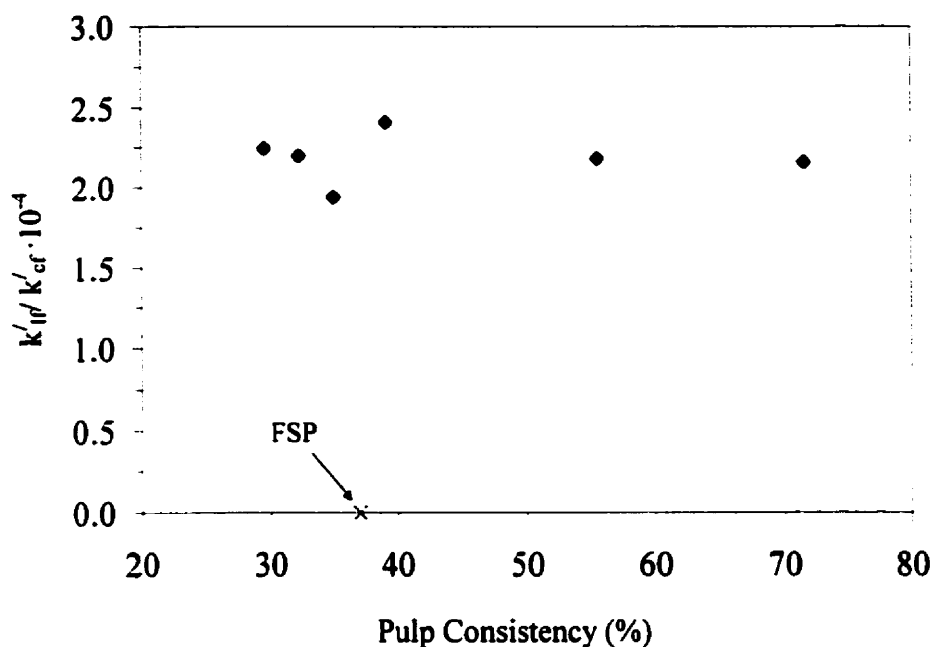


**Figure 4.7** Lignin-carbohydrate selectivity of ozone in cottonwood pulp.

occurs when the effect of shortening the diffusional path of ozone transport is dominated by the ever decreasing ECCSA.

The lignin-carbohydrate selectivity, calculated as the ratio of the rate of delignification and the rate of cellulose degradation ( $k'_{lf}/k'_{cf}$ ) is plotted as a function of consistency in Figure 4.7. It shows that the lignin-carbohydrate selectivity is independent of consistency for the consistency range of 30-70%. Since both delignification and cellulose degradation are governed by the same mechanism of ozone diffusion through the fibre wall their relative behaviour in the form of selectivity is not a function of consistency.

#### 4.3.2 Effect of Pulp Type

Zhang [14] has found that the rate of delignification during ozonation is proportional to the square root of the product of the initial kappa number and the ozone



partial pressure. The rate of cellulose chain scission is proportional to the ozone partial pressure to the power 0.6, but is not affected by the initial kappa number. Normalization of the delignification and cellulose chain scission rate data by taking into account the initial lignin content and the ozone partial pressure makes it possible to compare the behaviour of different pulp types. The normalized rates of delignification and cellulose degradation will be used in the remainder of this study and are represented by  $k'_{if} / (K_o \times P_o)^{0.5}$  and  $k'_{cf} / P_o^{0.6}$  respectively.

To determine the effect of pulp type (hardwood versus softwood) on the kinetics of ozone bleaching, three hardwood pulps (cottonwood, and two southern hardwoods with different initial kappa number) were compared with the data reported by Zhang [16] for Hemlock. All four pulps had undergone oxygen delignification.

The rates of delignification for these pulps are plotted as a function of pulp consistency in Figure 4.8. For each of the four pulp types the maximum rate of delignification occurred at a consistency higher than the fibre saturation point. It also shows that the normalized maximum delignification rate of cottonwood is higher than that of southern hardwood pulp, or Hemlock which are about the same.

Gandek [9] has found that the rate of delignification in the form of  $k'_{if}$  is inversely proportional to the average fibre wall thickness,  $w$  (m) as:

$$k'_{if} \propto \frac{\sqrt{K_o \cdot P_o}}{w} \quad (4.1)$$

Taking this dependency on fibre wall thickness into account, the experimental data of Figure 4.8 was replotted as  $k'_{if} w / (K_o \cdot P_o)^{0.5}$  in Figure 4.9. The x-axis was also modified to reflect the change in pulp consistency (%) relative to the FSP (%) for each pulp. It is

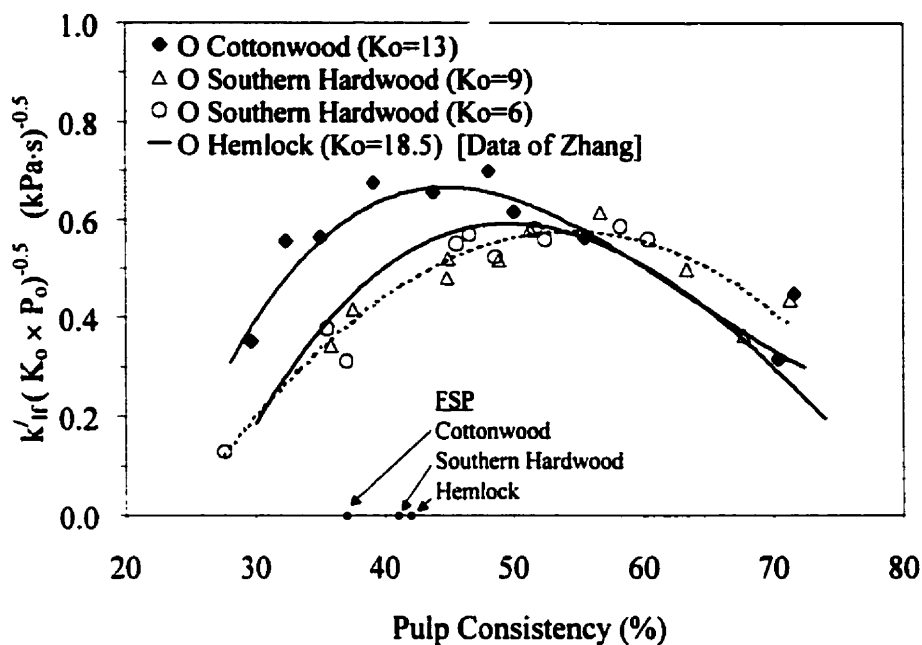


**Figure 4.8** The effect of Softwood versus hardwood on the rate of delignification.

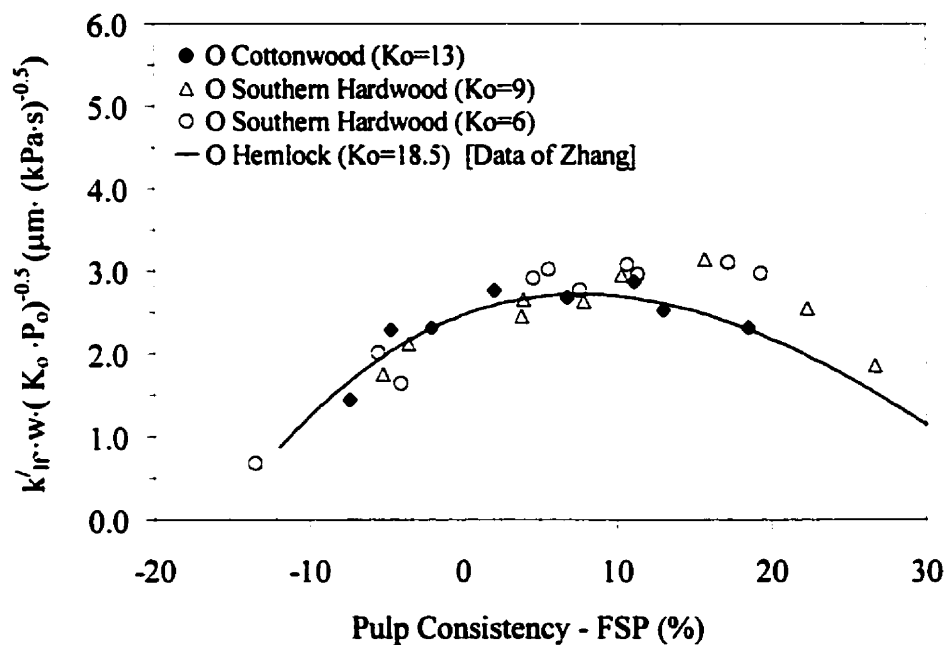


**Figure 4.9** Softwood and hardwood pulps are indistinguishable from one another with respect to the rate of delignification.

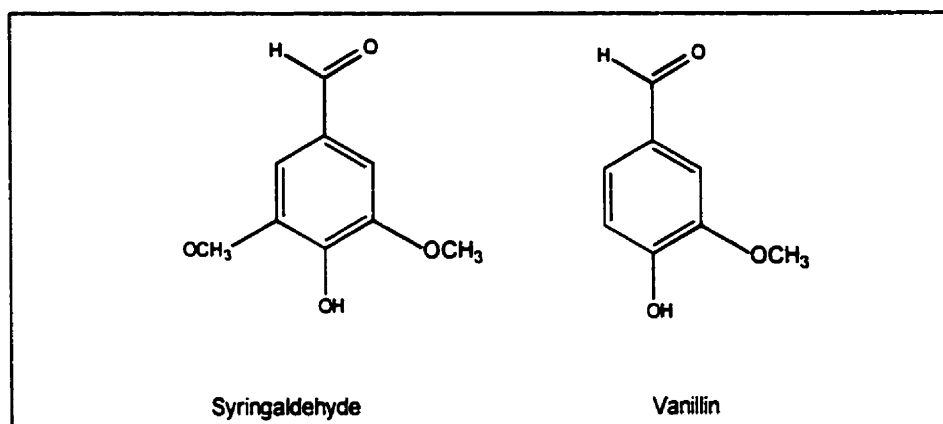


**Figure 4.10** Representative guaiacyl and syringyl components of lignin

evident from Figure 4.9 that with the additional corrections for the fibre width and the FSP that the four pulp types display virtually the same delignification behaviour. It also shows that the maximum rate of delignification is attained at a consistency about 10% greater than the fibre saturation point. This finding that the data in Figure 4.9 are very similar for hardwood and softwood fibres of widely different initial kappa numbers after appropriate corrections are made for  $K_o$ ,  $P_o$ ,  $w$  and FSP, provides strong support for the shrinking core model of delignification. It also implies that the rate of diffusion of ozone in hardwood and softwood cell walls is the same.

Although unimportant for the rate of delignification, the structure of lignin might be important for the cellulose degradation rate, since the radical yield is affected by certain functional groups. Ragnar has shown [18,19] that the extent of hydroxyl radical formation is determined by the relative amounts of certain acidic functional groups attached to the aromatic groups of lignin. Electron donating groups (OH, OR,  $NH_2$  etc.) enhance the reactivity of the aromatic structure towards ozone. Therefore, aromatic rings that are highly substituted with donor groups produce a substantial amount of radicals when they react with ozone. Syringyl components having an  $\alpha$ -carbonyl group produce a

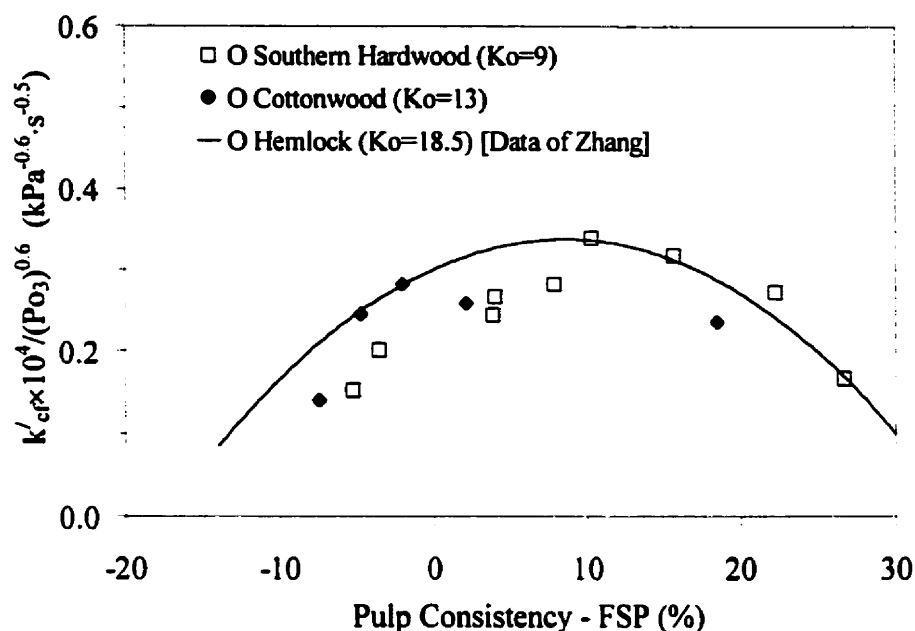


**Figure 4.11** The effect of softwood and hardwood on the rate of cellulose degradation.

yield of hydroxyl radicals twice its counterpart, which has an  $\alpha$ -methylene group in place of the  $\alpha$ -carbonyl. This is in spite of the fact that the  $\alpha$ -methylene substituted nuclei have a rate constant an order of magnitude higher than the  $\alpha$ -carbonyl substituted nuclei. Guaiacyl components having either an  $\alpha$ -carbonyl or an  $\alpha$ -methylene group react to produce approximately the same yield of hydroxyl radicals. Some lignin species containing guaiacyl nuclei react with ozone to produce a lower yield of radicals. Oxidation of the lignin components to  $\alpha$ -carbonyl function groups would increase the hydroxyl yield for syringyl but not guaiacyl containing compounds. The guaiacyl nuclei has one less electron withdrawing group than its syringyl equivalent making it less reactive towards ozone attack (Figure 4.10). It therefore has a lower radical yield than the syringyl nuclei.

Ragnar [18,19] has shown that the initial yield of radicals produced based on the amount of ozone consumed is approximately 12% for vanillin, an  $\alpha$ -carbonyl guaiacyl

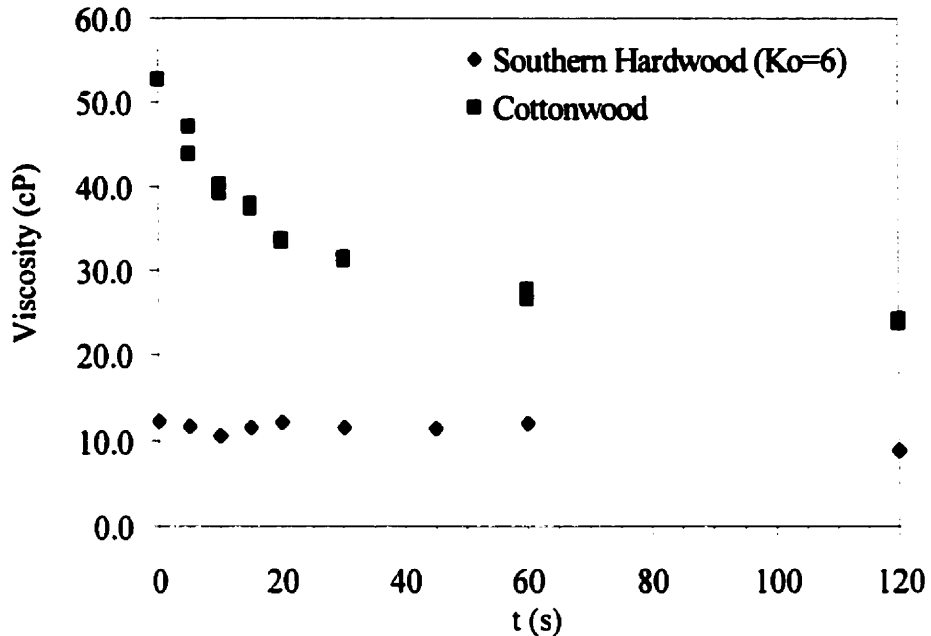


**Figure 4.12** A comparison of the typical shrinking core model behaviour of cottonwood with that of southern hardwood ( $K_o=6$ ).

compound, while it is 28% for syringaldehyde, an  $\alpha$ -carbonyl syringyl component. Accordingly the cellulose degradation in hardwood fibres is expected to be larger than that of softwood fibres.

The effect of hardwood versus softwood on the rate of cellulose degradation is presented in Figure 4.11 for cottonwood, southern hardwood ( $K_o=9$ ) and Hemlock pulp. The southern hardwood with a lower kappa number ( $K_o=6$ ) was not considered as the starting viscosity was too low. Regardless of ozonation time, the number of cellulose chain scission in the southern hardwood ( $K_o=6$ ) remained essentially constant. For this reason the effect of consistency on the rate of cellulose degradation could not be determined. A comparison of this behaviour with that of cottonwood is illustrated in Figure 4.12. A possible explanation for this behaviour is that the initial viscosity is too

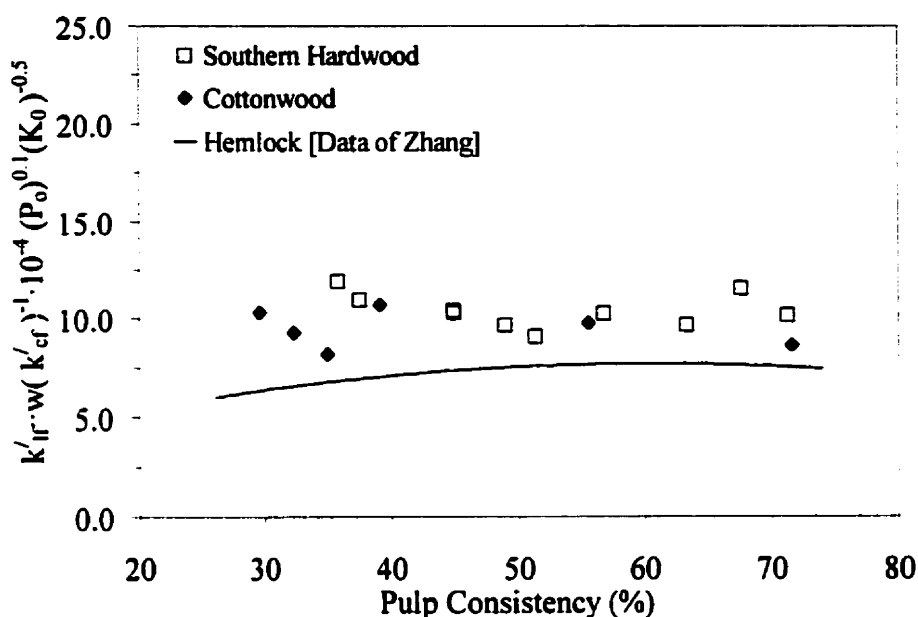


**Figure 4.13** Ozone is more selective in hardwood pulps than in softwood pulps.

low so that further cellulose degradation cannot be characterized properly with the present method of viscometry and choice of viscometer.

It can be seen that the normalized cellulose degradation data of the two hardwood fibres are not much different from that of Hemlock, contrary to expectation based on the radical yield results of Ragnar [18]. The explanation might be that the residual lignin in the hardwood species is quite different from that in the original wood after the many preceding delignification stages.

The lignin-cellulose selectivity of the different hardwood and softwood pulps can be compared when the appropriate corrections are made for the initial kappa number, ozone pressure and the fibre wall thickness, i.e. the normalized selectivity was defined as:

$$\frac{k'_f \times w}{k'_{cf}} \times 10^2 \frac{(P_o)^{0.1}}{(K_o)^{0.5}} \quad (4.2)$$

The normalized selectivity for southern hardwood, cottonwood and Hemlock is plotted in Figure 4.13 versus pulp consistency. It can be seen that the normalized selectivity is independent of consistency and that the Hemlock softwood is less selective than the two hardwoods.

### **4.3.3 Effect of Pre-Bleaching Treatment**

The effect of peroxide pre-bleaching on the normalized rates of delignification during ozonation is shown in Figure 4.14. It can be seen that there is no significant difference between the rate of delignification of O and OP southern pine. This indicates that the pre-oxidation of the lignin prior to ozone treatment has no effect on the kinetics of lignin removal during ozone bleaching. Both observations are further evidence that the structure of lignin is not important for delignification kinetics. The normalized rate of cellulose degradation of O and OP southern pine is shown in Figure 4.15. The results indicate that the pre-treatment with peroxide leads to a higher rate of cellulose chain scission. The explanation might be that the peroxide introduces carbonyl groups in the side chain of lignin which enhances the hydroxyl radical yield [18].

The normalized rates of delignification, cellulose degradation and the lignin-carbohydrate selectivity for ozone treatment of all the different pulps are summarized in Figures 4.16, 4.17 and 4.18.

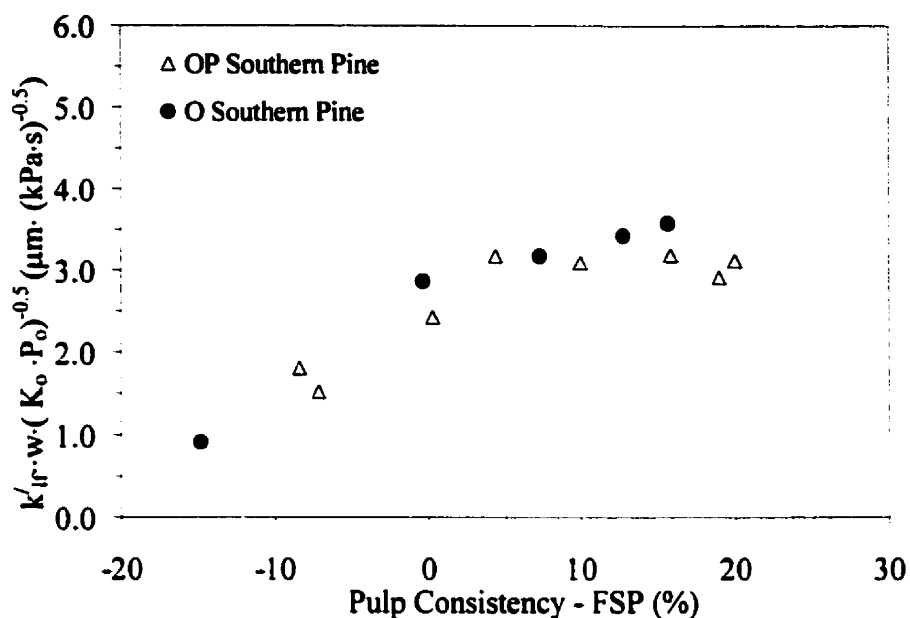


**Figure 4.14** Effect of pre-treatment on the rate of delignification. O versus OP pre-bleached pulp.

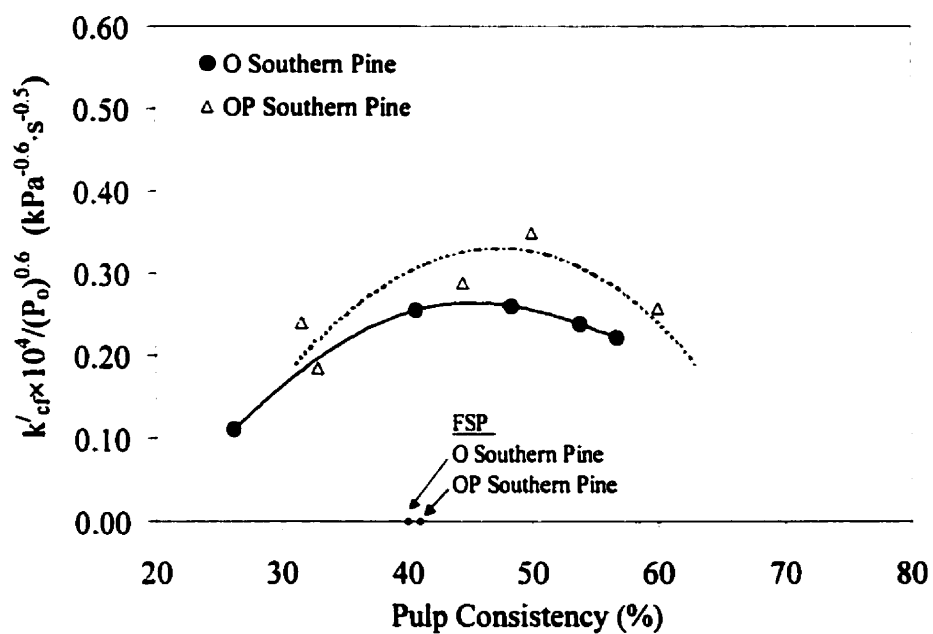


**Figure 4.15** Pre-treatment with peroxide accelerates the rate of cellulose chain scission during ozone bleaching.

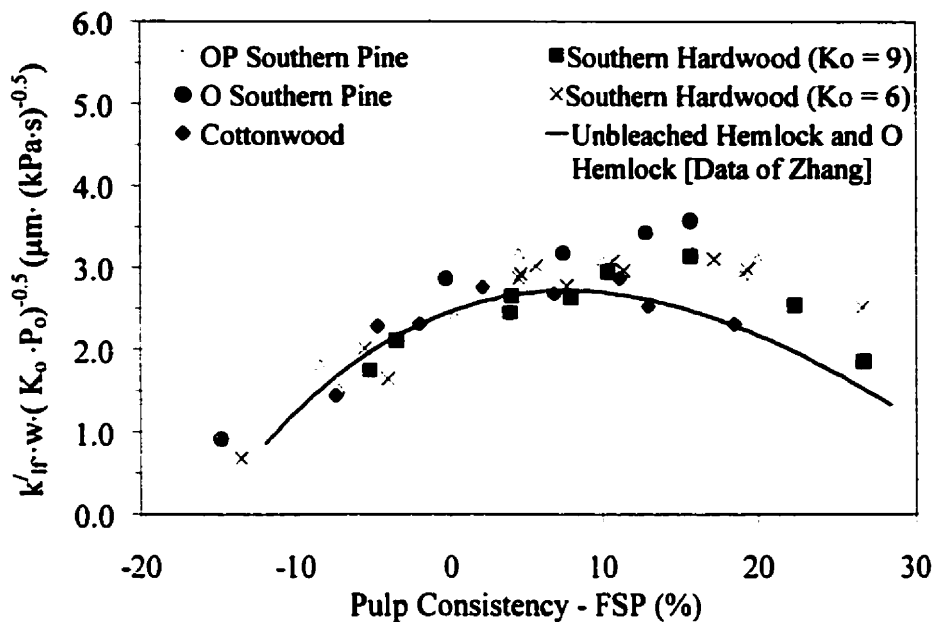


It is obvious from Figures 4.16 and 4.17 that for all pulp types regardless of species or pre-bleaching treatment, the normalized rates of delignification and cellulose degradation are generally quite comparable although the differences are somewhat larger for the cellulose degradation. These two figures also show that the maximum rates occur at a consistency higher than the FSP. According to Zhang [24], the maximum rate of delignification and cellulose degradation occur at 50% consistency for Hemlock kraft pulp, which is 8% higher than its fibre saturation point of 42%. The consistencies at which the normalized rates of the pulp types studied reach their maximum are listed in Table 4.2. It shows that the maxima occur at roughly the same consistency for the delignification and cellulose degradation for all the pulp types investigated. It can be seen that the maxima occur at a consistency about 10% greater than the fibre saturation point of each pulp types.

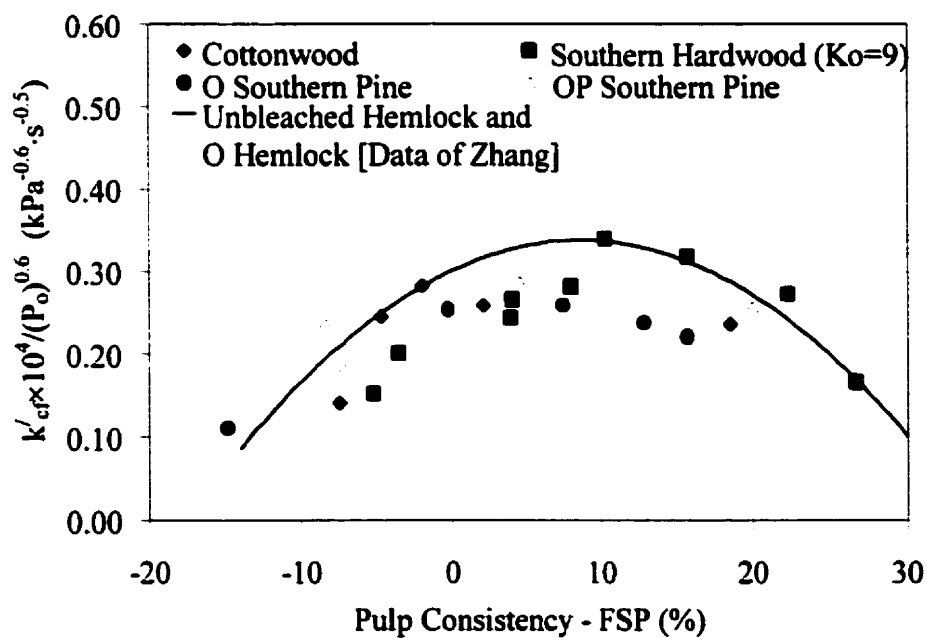
Finally, it is evident from Figure 4.18 that the normalized selectivity is not affected by consistency. The Hemlock pulp appears to be less selective than those studied in the present investigation, and peroxide pre-bleaching decreases the selectivity for southern pine.

TABLE 4.2 Relationship between fibre saturation point and maximum rates

Pulp Type	FPS% ( $\pm 2\%$ )	Approximate Maximum Rate of		Max rate-FSP
		Delignification	Cellulose Degradation	
Cottonwood	37	45	45	8
Southern Hardwood ( $K_o=9$ )	41	51	51	10
Southern Hardwood ( $K_o=6$ )	41	53	-	12
OP Southern Pine	40	49	49	9
O Southern Pine	41	6	8	7
Unbleached Hemlock (data of Zhang [23])	42	50	50	8



**Figure 4.16** Effect of pulp consistency on delignification



**Figure 4.17** Effect of pulp consistency on cellulose degradation

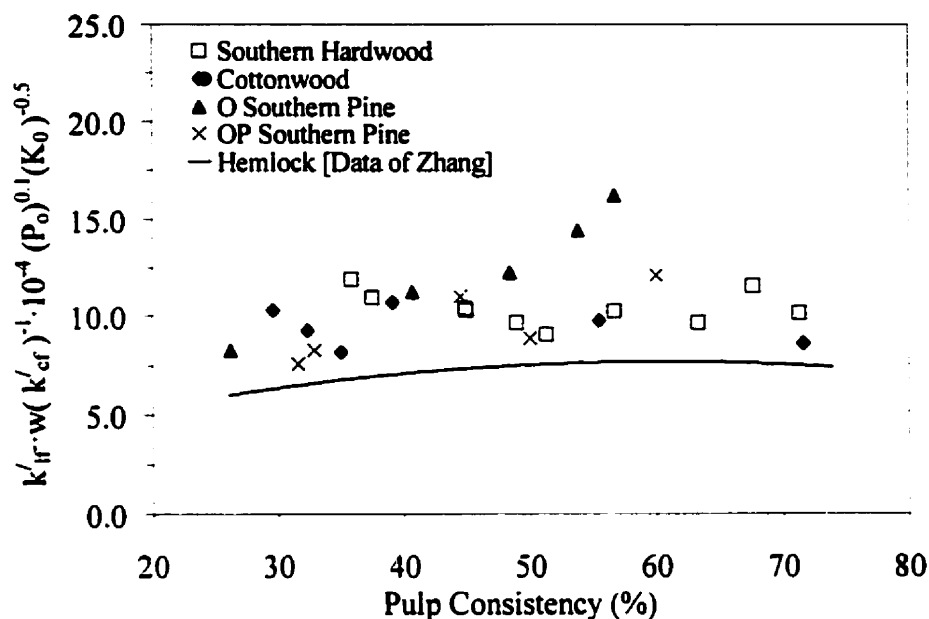


**Figure 4.18** The lignin-carbohydrate selectivity of ozone for all pulp types studied.

#### 4.4 CONCLUSIONS

The maximum rates of delignification and cellulose degradation for all species studied occur at a consistency about 10% greater than the fibre saturation point. The rates of delignification when normalized with respect to initial kappa number, ozone partial pressure and average fibre wall width are approximately the same for softwoods and hardwoods, and also not significantly influenced by bleaching sequence preceding the ozonation. This behaviour is consistent with the shrinking core model of delignification by ozone which requires that the kinetics are governed by diffusion in the fibre wall and not by the lignin structure.

The rate of cellulose degradation appears to be somewhat dependent on the chemical nature of the lignin. It is found that peroxide pre-treatment leads to a higher rate of cellulose degradation. With regards to the normalized lignin-cellulose selectivity the data shows that Hemlock is less selective than the hardwood and softwood species

investigated in the present study. Peroxide pre-bleaching decreases the selectivity for southern pine.

## **CHAPTER 5**

### **PREDICTION OF THE RATES OF DELIGNIFICATION AND CELLULOSE DEGRADATION DURING OZONATION**

#### **5.1 INTRODUCTION**

In agreement with Zhang et al. [14] and Gandek [9] it was shown in Chapter 4 that the initial delignification period during ozone bleaching of pulp follows a “shrinking core” model with diffusion of ozone through the reacted fibre wall region being the rate-determining step. The effect of operating parameters such as ozone partial pressure, initial kappa number and consistency on the rate processes was well described by this theory for the different wood pulp species investigated in the present study. Gandek [9] showed that the rate of delignification is inversely proportional to the average fibre wall thickness. Most recently, Bennington et al. [13] were able to model numerically the delignification for Hemlock kraft pulp over the entire reaction period using the shrinking core model when the fibre wall thickness distribution is taken into consideration.

In the present chapter the effect of consistency on delignification and cellulose degradation is described based on the shrinking core model. A simplified method is also presented to take into account the effect of the fibre wall thickness distribution on the different periods of delignification. This is followed by the testing of Gandek’s expression for the rate of delignification and a similar expression for the cellulose degradation rate for the six different pulp types investigated in this study. Finally it is evaluated whether all the rate data generated in this study can be described by generalized delignification and cellulose degradation curves which are solely based on the physical and chemical properties of the pulp.

## 5.2 THEORY

### 5.2.1 Generalized Expression for $\frac{\Delta K}{K_o}$ and $\frac{1}{DP_t} - \frac{1}{DP_o}$

It has been shown by Zhang [24] that the rate constant of delignification ( $k'_{if}$ ) during ozonation can be described as;

$$k'_{if} = 1.5 \left( \frac{[O_3]^* D_m \rho_l}{m[L]_o w_{co}^2 \rho_w^2} \right)^{1/2} \left( \frac{c \times ECCSA}{100 - c} \right)^{1/2} (\Delta K)_{Lumen} \quad (5.1)$$

where  $[O_3]^*$  is the saturated ozone concentration ( $\text{kmol/m}^3$ ) in the liquid,  $D_m$  is the molecular diffusion coefficient ( $\text{m}^2/\text{s}$ ) of ozone in the impregnation liquid,  $m$  is the stoichiometry ( $\text{kmol/kg}$  lignin) of the fast lignin-ozone reactions,  $[L]_o$  is the lignin content ( $\text{kg}$  lignin/ $\text{kg}$  pulp) of unbleached pulp,  $w_{co}$  is the fully collapsed fibre wall thickness of the thinnest fibres ( $\text{m}$ ),  $\rho_w$  is the solid wood density ( $\text{kg}$  pulp/ $\text{m}^3$ ),  $\rho_l$  is the impregnation liquor density ( $\text{kg/m}^3$ ),  $c$  is the pulp consistency (%), ECCSA is the ratio of effective diffusivity ( $D_e$ ) and the molecular diffusivity ( $D_m$ ) called the Effective Capillary Cross Sectional Area, and  $(\Delta K)_{Lumen}$  is the total change in kappa number up to the end of the initial regime.

With  $\Delta K = k'_{if} \sqrt{t}$  and knowing that about 2% (on pulp) ozone consumption removes 20 kappa units [5],  $m[L]_o$  becomes  $0.001K_o$  ( $\text{kg O}_3/\text{kg o.d. pulp}$ ) and Equation 5.1 becomes

$$\frac{\Delta K}{K_o} = \alpha \left( \frac{P_o \times t}{K_o \times w_{co}^2} \right)^{1/2} \left( \frac{c \times ECCSA}{100 - c} \right)^{1/2} \frac{(\Delta K)_{Lumen}}{K_o} \quad (5.2)$$

where  $\alpha$  is a constant,  $\Delta K = K_o - K_t$ ,  $K_o$  is the initial kappa number of the pulp, and  $K_t$  is the kappa number of the pulp after ozonation time.

Beyond the fibre saturation point, the ECCSA is strongly dependent on the consistency of the pulp and is inversely proportional to the tortuosity,  $\lambda$ , according to [23]

$$\text{ECCSA} = \frac{\varepsilon}{\lambda} = \frac{1}{\lambda} \left( \frac{1}{1 + \frac{\rho_l}{\rho_w} \left( \frac{c}{100-c} \right)} \right) \quad (5.3)$$

The tortuosity value for a pulp is constant below the fibre saturation point due to the swollen state of the pulp fibres. It remains constant up to a consistency of approximately 10% above the fibre saturation point [24]. The ratio of impregnation liquor density to solid wood density is constant ( $\rho_l/\rho_w = 1/1.5 = 0.67$ ), therefore equation 5.3 can be combined with 5.2 to yield

$$\frac{\Delta K}{K_o} = \alpha \cdot \left( \frac{P_o \times t}{K_o \times w_{CO}^2} \right)^{1/2} \left( \frac{c}{100-c+0.67c} \right)^{1/2} \frac{(\Delta K)_{\text{Lumen}}}{K_o} \quad (5.4)$$

$$= \alpha \cdot \left( \frac{P_o \times t \times c}{K_o \times w_{CO}^2 (100-0.33c)} \right)^{1/2} \frac{(\Delta K)_{\text{Lumen}}}{K_o} \quad (5.4b)$$

where  $\alpha'$  is the modified proportionality constant.

Equation 5.4 enables the prediction of the extent of kappa number reduction during ozonation based on easily measured system parameters. According to the work of Zhang [5],  $(\Delta K)_{\text{Lumen}}$  is a constant at  $0.6K_o$ . The thickness of the fully collapsed fibre wall is not easily determined but it is related to the thickness of the fully swollen fibre wall according to

$$w_{co} = w_o (1 - \varepsilon_{\text{FSP}}) \quad (5.5)$$

where  $\varepsilon_{\text{FSP}}$  is the void fraction of the pulp at the fibre saturation point and  $w_o$  is the fully swollen fibre wall thickness (m). The void fraction,  $\varepsilon$ , at any pulp consistency can be written as

$$\varepsilon = \frac{1}{1 + \frac{\rho_l}{\rho_w} \left( \frac{c}{100-c} \right)} = \frac{1}{1 + 0.67 \left( \frac{c}{100-c} \right)} = \frac{100-c}{100-0.33c} \quad (5.6)$$

Therefore at the fibre saturation point, where the pulp consistency,  $c$ , is the fibre saturation point FSP(%)

$$\varepsilon_{\text{FSP}} = \frac{100 - \text{FSP}}{100 - 0.33\text{FSP}} \quad (5.7)$$

Substituting Equation 5.7 into 5.5 yields a relationship for the fully collapsed fibre wall thickness in terms of the FSP, a parameter characteristic of an individual pulp

$$w_{\text{co}} = w_o \left( \frac{0.67\text{FSP}}{100 - 0.33\text{FSP}} \right) \quad (5.8)$$

Using this relationship Equation 5.4 can be rearranged into a relationship that describes the effect of pulp consistency on the rate of delignification during ozonation as

$$\frac{\Delta K}{K_o} = \alpha \cdot \left( \frac{100 - 0.33\text{FSP}}{\text{FSP} \times w_o} \right) \times \left( \frac{P_o \times c \times t}{K_o (100 - 0.33c)} \right)^{1/2} \times \frac{(\Delta K)_{\text{Lumen}}}{K_o} \quad (5.9)$$

This generalized relationship describing the rate of delignification is based solely on the physical and chemical properties of the pulp. A similar generalized relationship describing the rate of cellulose degradation

$$\frac{1}{\text{DP}_t} - \frac{1}{\text{DP}_o} = \Delta \left( \frac{1}{\text{DP}} \right) = \beta \cdot \left( \frac{100 - 0.33\text{FSP}}{\text{FSP} \times w_o} \right) \times P_o^{0.1} \times \left( \frac{P_o \times c \times t}{(100 - 0.33c)} \right)^{1/2} \quad (5.10)$$

can be derived starting from the equation of that describes the rate constant of cellulose chain scission ( $k'_{\text{cf}}$ ) during ozonation [24] as;



$$k'_{cf} = k \left( \frac{[O_3]^{(1.2)} D_m \rho_l}{mw_{CO}^2 \rho_w^2} \right)^{1/2} \left( \frac{c \times ECCSA}{100 - c} \right)^{1/2} \quad (5.11)$$

where  $k$  is the proportionality constant for cellulose chain scission.

### 5.2.2 Determination of $w_o$ and $(\Delta K)_{Lumen}$

During the initial regime of ozonation, the rate of delignification starts to decrease when the ozone-lignin reaction front has penetrated the fibres. As ozonation time increases, the ozone-lignin reaction front reaches the lumen of the thinner fibres. At this point the total kappa number decrease during ozonation is  $(\Delta K)_{Lumen}$ . During the following transition regime the reaction front reaches the lumen of progressively thicker fibres, further slowing down the rate of delignification of the pulp. Lastly, during the final regime of ozonation the majority of fibres have been fully delignified and the ozone-lignin reaction rate becomes zero.

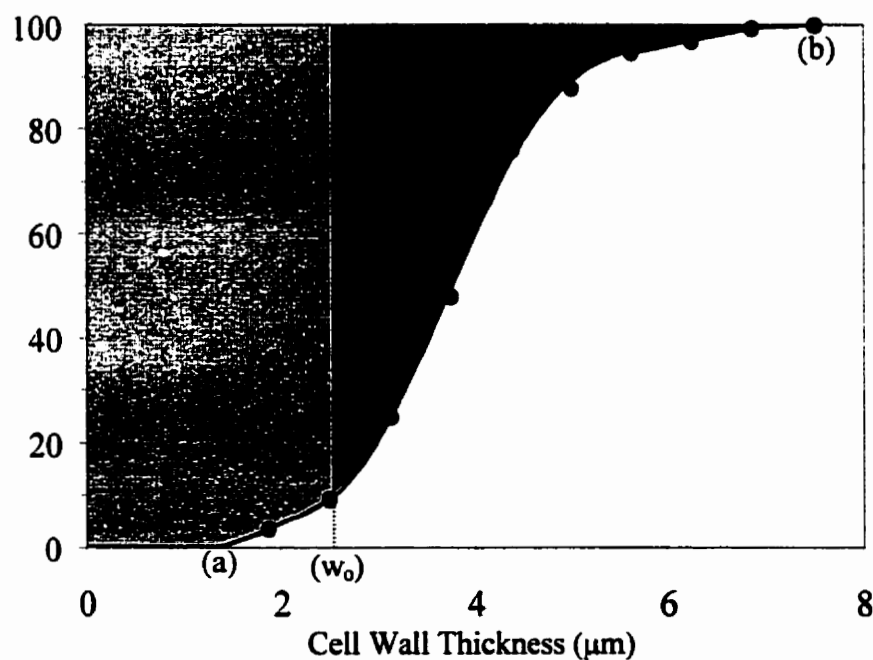
In order use Equations 5.9 and 5.10 it is necessary to define the wall thickness of the thinnest fibres,  $w_o$  and  $(\Delta K)_{Lumen}$ . The thinnest fibre wall thickness was somewhat arbitrarily defined as the fibre wall width that corresponds to the thinnest 10% of the cumulative fibre width distribution. For consistent determination of  $(\Delta K)_{Lumen}$  for the different pulp types a method was devised which relates  $(\Delta K)_{Lumen}$  directly to  $w_o$ . The method assumes that  $(\Delta K)_{Lumen}$  is reached when the reaction front has reached the lumen of the fibres with a wall thickness of  $w_o$ .

Figure 5.1 shows that cumulative fibre width distribution for cottonwood. Assuming that all the fibres have the same fibre length and lignin concentration (g lignin/volume of fibre wall) it follows that

$$\frac{(\Delta K)_{\text{Lumen}}}{K_0} \propto \frac{\int_0^{w_n} (100 - y) dw}{\int_0^{w_f} (100 - y) dw} \quad (5.12)$$

where  $w_0$  is the thickness represented by the 10% cumulative fibre wall thickness distribution,  $w_f$  is the fibre wall thickness of the thickest fibres wall,  $w$  is the fibre wall thickness, and  $y$  represents the cumulative fibre width distribution in percentage.

This particular situation whereby the total lignin removal,  $\Delta K$ , is equal to  $K_{\text{Lumen}}$  is represented in Figure 5.1. The lighter area represents the cumulative amount of lignin removed in the time it take the reaction front to reach the lumen of the 10% thinnest fibres, while the darker area is the total amount of lignin still remaining in the thicker fibre walls.



**Figure 5.1** Determination of  $(\Delta K)_{\text{Lumen}}$  by integration of the cumulative fibre wall width distribution of cottonwood.

It can be seen in Figure 5.1 that for cottonwood  $w_o=2.63$ , and that the ratio of the lighter area and the total (lighter + darker) area is 0.63, i.e.  $(\Delta K)_{Lumen} = 0.63 K_o$ . The values of  $w_o$  and  $(\Delta K)_{Lumen}$  are summarized in Table 5.1. With the determination of  $(\Delta K)_{Lumen}$  from the cumulative fibre wall width distribution the rates of delignification and cellulose degradation described by Equations 5.9 and 5.10 respectively can be related directly to solely measurable physical and chemical parameters of the ozone-pulp system.

Table 5.1 Determination of the extent of delignification at optimum ozone delignification

Pulp Type	$K_o$ (kappa)	$w_o$ ( $\mu\text{m}$ )	$(\Delta K)_{Lumen}$ (kappa)	$\frac{(\Delta K)_{Lumen}}{K_o}$
Cottonwood	13	2.56	8.2	0.63
Southern Hardwood	9	2.82	5.1	0.57
Southern Hardwood	6	3.10	3.7	0.62
OP Southern Pine	15	2.75	7.8	0.52
O Southern Pine	14	2.71	7.0	0.50
Unbleached Hemlock [data of Zhang [5)]	31	2.56	18.5	0.6

### 5.3 SIMPLIFIED PREDICTIVE APPROACH

Assuming that the lignin is uniformly distributed throughout the cell wall and that the shrinking core model applies, Gandek [9] reasoned that a change in kappa number would be proportional to the ratio of the penetration distance of the ozone-lignin reaction front,  $\delta$ , and the average cell wall thickness,  $\bar{w}$ .

$$\Delta K = K_o \frac{\delta}{\bar{w}} \quad (5.13)$$

The shrinking core model predicts that the location of the ozone-lignin reaction front within the fibre wall is dependent on the ozonation time, the concentration of ozone and the concentration of lignin in the fibre wall according to

$$\delta \propto \left( \frac{P_o t}{K_o} \right)^{1/2} \quad (5.14)$$

Combining Equations 5.13 and 5.14 with the rate equation of delignification  $\Delta K = k'_{if} (P_o \times t)^{1/2}$  results in an equation defining the rate of delignification during the initial regime of ozonation as

$$k'_{if} = K_G \frac{\sqrt{K_o}}{\bar{w}} \quad (5.15)$$

Therefore the change in kappa number during the initial regime of ozonation can be predicted by

$$\Delta K = \frac{K_G}{\bar{w}} (K_o P_o t)^{1/2} \quad (5.16)$$

where  $K_G$  is the proportionality constant called the Gandek constant.

The consistency of a pulp during ozonation has a strong effect on the rate of delignification. It has been shown in Chapter 4 that the rate of delignification for each pulp type can be readily compared at their respective fibre saturation point (FSP). At the FSP the pulp fibre wall is fully swollen, and all the available water can just be accommodated in the fibre wall pore structure. By evaluating Equation 5.16 at the FSP of the pulps the effect of consistency is eliminated. This simplified predictive model is applicable at the FSP and is valid in describing only the initial regime of ozonation.

By using ozone kinetics data available for Hemlock kraft pulp at its fibre saturation point [5], Gandek found the proportionality constant to be 1.6 [9]. Using the initial lignin content, the average water saturated fibre wall thickness as measured by Econotech, and the obtained value of  $k'_{if}$  at the FSP, the Gandek constant was calculated

for the different pulp types. It can be seen in Table 5.2, that the Gandek constant is about 1.6 for all pulp types except O southern pine which has a value of 2.1.

**Table 5.2** Gandek Constant as determined at the fibre saturation point

Pulp Type	$K_o$ (kappa)	$k'_{ir}$ (kappa $\times$ s <sup>-0.5</sup> )	$\bar{w}$ ( $\mu$ m)	$K_G$ $\left( \frac{\mu\text{m}}{(\text{kappa} \times \text{kPa} \times \text{s})^{0.5}} \right)$
Cottonwood	13	1.4	4.1	1.6
Southern Hardwood	9	0.95	5.1	1.6
Southern Hardwood	6	0.8	5.3	1.7
OP Southern Pine	15	1.1	5.7	1.6
O Southern Pine	14	1.4	5.7	2.1
Unbleached Hemlock (data of Zhang [5])	31	1.9	4.6	1.6

#### 5.4 TORTUOSITY AND ECCSA

Zhang [5] developed the following relationship between the ECCSA and the rate of delignification at consistencies above the fibre saturation point (see Chapter 2).

$$\text{ECCSA} = \left( \frac{k'_{ir}}{(\Delta K)_{\text{Lumen}}} \right)^2 \left( \frac{m[L]_o w_{c0}^2 \rho_w^2}{[O_3]^* D_m \rho_l} \right) \left( \frac{100-c}{c} \right) \quad (5.17)$$

where  $k'_{ir}$  is the rate constant of delignification,  $m$  is the stoichiometry (kmol/kg lignin) of the fast ozone-lignin reactions,  $[L]_o$  is the initial lignin content (kg lignin/ kg pulp) before ozone treatment,  $w_{c0}$  is the fully collapsed fibre wall thickness of the thinnest 10% of the fibres (m),  $\rho_w$  is the solid wood density (kg pulp/m<sup>3</sup>),  $\rho_l$  is the impregnation liquor density (kg/m<sup>3</sup>),  $[O_3]^*$  is the saturated ozone concentration (kmol/m<sup>3</sup>) in the impregnation liquid,  $D_m$  is the molecular diffusion coefficient (m<sup>2</sup>/s) of ozone in the impregnation liquid, and  $c$  is the pulp consistency (%).

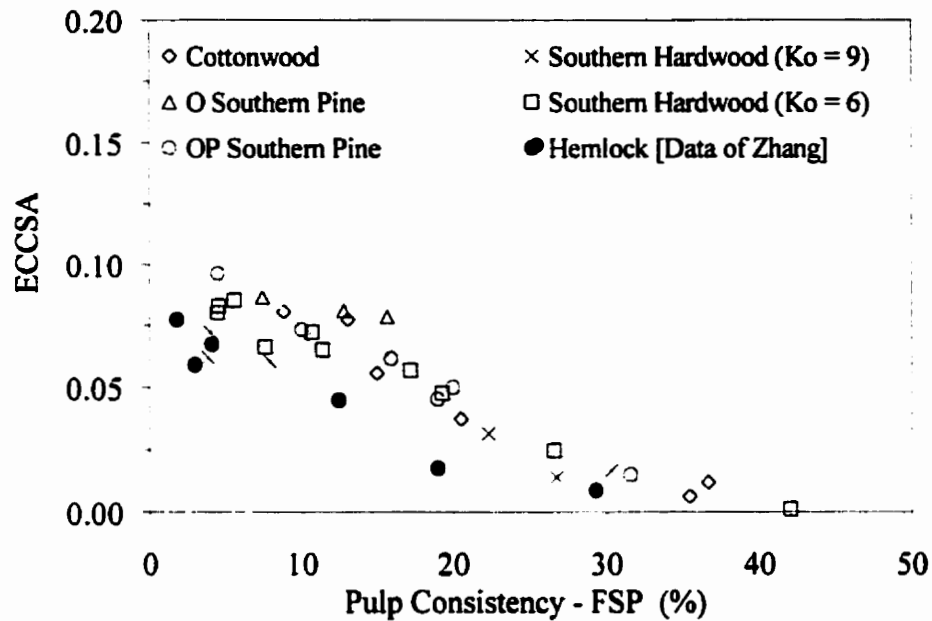


**Figure 5.2** Effective Capillary Cross-Sectional Area (ECCSA)

At consistencies equal to or below the fibre saturation point for a given pulp, the pulp fibres are in a completely swollen state, containing the maximum amount of water that a fibre can hold within the fibre walls. Therefore, below the fibre saturation point only the amount of water outside the pulp fibres increases with decreasing consistency. Since the ECCSA of a fibre quantifies the effective diffusional transport of ozone through the fibre relative to molecular diffusion of ozone in a homogeneous impregnation solution, the value of ECCSA will remain constant below the fibre saturation point. Increasing the consistency beyond the fibre saturation point decreases the amount of water contained within the fibre, thereby decreasing the effective diffusion of the ozone, and thus the ECCSA.

To calculate the ECCSA for each pulp type, the following values and parameters were used. Zhang [5] found that 2% (on pulp) ozone consumption removed about 20 kappa units therefore  $m[L]_0$  becomes  $0.001K_0$ . The thinnest fibre wall thickness,  $w_0$ , of

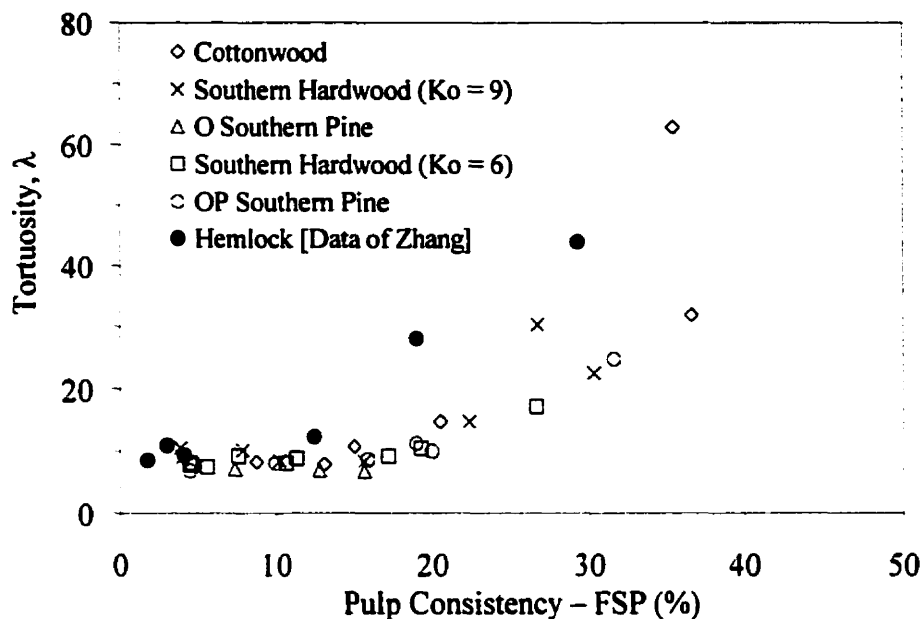


**Figure 5.3** Tortuosity of the fibres

Table 5.1, was used to calculate the value of the fully collapsed fibre wall thickness,  $w_{co}$ , according to  $w_{co} = w_o(1 - \varepsilon_{FSP})$ , with  $\varepsilon_{FSP}$  defined by Equation 5.7.

The initial lignin content,  $K_o$ , and  $(\Delta K)_{Lumen}$  are also taken from Table 5.1,  $\rho_w$  is taken to be  $1500 \text{ kg/m}^3$  and  $\rho_l$  as  $1000 \text{ kg/m}^3$ . According to Zhang [5],  $D_m$  for ozone diffusion in acidified water at  $10^\circ\text{C}$  is  $1.29 \times 10^{-9} \text{ m}^2/\text{s}$ . Combining the above parameters with the rate of delignification ( $k'_{lf}$ ) at the various pulp consistencies, the ECCSA above the fibre saturation point for each pulp type can be determined. Similarly the tortuosity,  $\lambda$ , was calculated from the ECCSA as  $\lambda = \varepsilon / \text{ECCSA}$ . The tortuosity is defined as the dimensionless length of the diffusional path of a chemical in the thickness direction of the fibre wall.

The results obtained for these calculations of ECCSA and  $\lambda$  are shown in Figures 5.2 and 5.3 respectively. It can be seen in Figure 5.2 that at consistencies near the fibre

saturation point the value of ECCSA decreases from a maximum value of about 0.07 to essentially zero at a consistency of about 40% above the FSP. Correspondingly,  $\lambda$  increases exponentially with the increasing consistency as a result of pore closure at the higher consistencies. The values of ECCSA and  $\lambda$  below the fibre saturation point can be taken to be equal to those at the FSP because the swollen state of the fibres remains the same as that at the fibre saturation point.

The trend of the curves in Figures 5.2 and 5.3 are in agreement with those developed by Zhang [5] in his study of oxygen delignified and unbleached Hemlock kraft pulp. Zhang calculated a value of 7 for tortuosity at the fibre saturation point of Hemlock pulps. The value calculated for the six pulp types, including the Hemlock data of Zhang, in this study is 9, which is somewhat higher. Zhang used a value of 1  $\mu\text{m}$  for the fully collapsed fibre wall thickness. However, in this study the thickness of the fully collapsed fibre wall of the thinnest 10% fibres for Hemlock was taken to be 0.85  $\mu\text{m}$ . This smaller fibre wall thickness resulted in a value of 10 for tortuosity of Hemlock kraft pulp fibres.

## 5.5 GENERALIZED CURVES OF DELIGNIFICATION AND CELLULOSE DEGRADATION

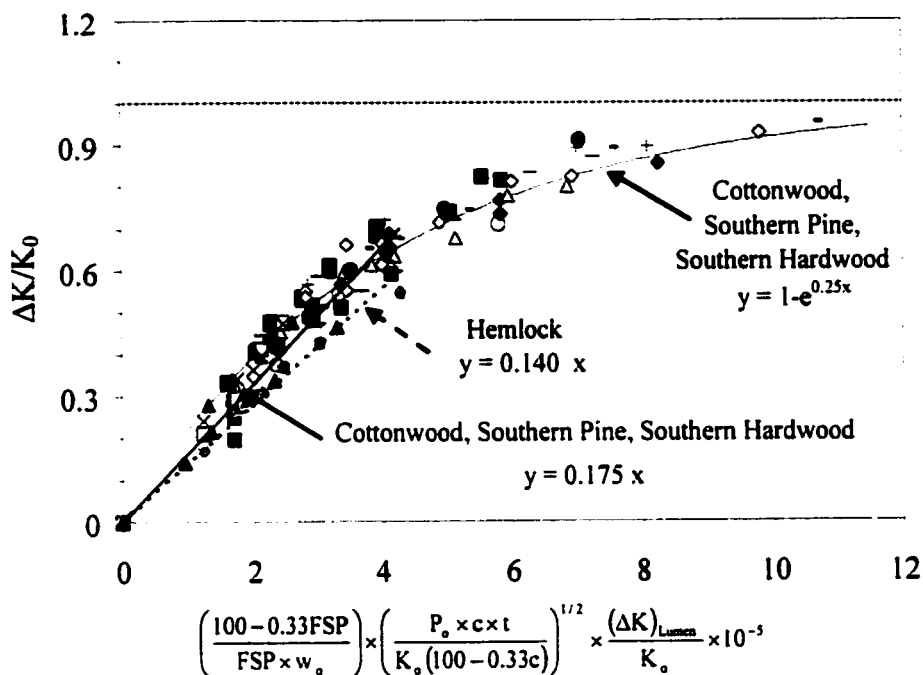
The generalized curves of delignification and cellulose degradation are represented respectively as:

$$\frac{\Delta K}{K_o} = \alpha \cdot \left( \frac{100 - 0.33\text{FSP}}{\text{FSP} \times w_o} \right) \times \left( \frac{P_o \times c \times t}{K_o (100 - 0.33c)} \right)^{1/2} \times \frac{(\Delta K)_{\text{Lumen}}}{K_o} \quad (5.9)$$

$$\Delta \left( \frac{1}{\text{DP}} \right) = \beta \cdot \left( \frac{100 - 0.33\text{FSP}}{\text{FSP} \times w_o} \right) \times P_o^{0.1} \times \left( \frac{P_o \times c \times t}{(100 - 0.33c)} \right)^{1/2} \quad (5.10)$$



Using the data described in Chapter 4 and values of  $w_0$  and  $(\Delta K)_{Lumen}$  listed in Table 5.1, a general relationship between the fractional degree of delignification,  $\Delta K/K_0$ , and time corrected for the ozone partial pressure and physical properties of the



- |                                    |  |
|------------------------------------|--|
| ◆ Cottonwood 39.1%                 | ◇ Southern Hardwood (Ko = 6) 45.6%             |
| ■ Southern Hardwood (Ko = 9) 45%   | □ OP Southern Pine 44.5%                       |
| △ Southern Hardwood (Ko = 9) 51.3% | ▲ OP Southern Pine 50%                         |
| ○ Southern Hardwood (Ko = 9) 48.9% | × O Southern Pine 48.4%                        |
| · Southern Hardwood (Ko = 9) 44.9% | ● O Hemlock                                    |
| ● Southern Hardwood (Ko = 6) 45.5% | — Unbleached Hemlock                           |
| ○ Southern Hardwood (Ko = 6) 46.6% | — Cottonwood, Southern Pine, Southern Hardwood |
| - Southern Hardwood (Ko = 6) 51.7% | ···· Hemlock                                   |
| - Southern Hardwood (Ko = 6) 48.6% |  |

**Figure 5.4** Generalized curve of delignification

pulp fibre can be developed (see Figure 5.4). From Figure 5.4 it once again is evident that the initial stage of delignification is linear with respect to the square root of ozonation time. At longer ozonation times the rate of lignin removal slows down, and eventually the delignification reaches an asymptotic plateau.

From a statistical evaluation of the data for all pulp types it appears that a generalized relationship can be established (99 times out of 100) that cottonwood, southern hardwood ( $K_o=9$ ), southern hardwood ( $K_o=6$ ), O southern pine and OP southern pine all can be described by the same relationship of

$$\frac{\Delta K}{K_o} = 0.175 \left( \frac{100 - 0.33FSP}{FSP \times w_o} \right) \times \left( \frac{P_o \times c \times t}{K_o (100 - 0.33c)} \right)^{1/2} \times \frac{(\Delta K)_{Lumen}}{K_o} \quad (5.18)$$

for the initial delignification regime. Only the Hemlock pulps (oxygen delignified and unbleached) have a behaviour significantly different from that of the other pulps, and delignify slower than the other pulps under the same ozonation conditions.

The slope of the linear portion of the generalized curve of delignification (Figure 5.4) represents the constant  $\alpha$  of Equation 5.9. The relationship 5.18 established for all the pulp types with the exception of Hemlock, holds up until approximately 50-60% delignification for each pulp species. Therefore the time to reach optimum ozonation can be predicted knowing only the operation condition of the ozonation system and the physical characteristics of the pulp. The extent of delignification beyond the optimum level of  $(\Delta K)_{Lumen} / K_o$  can be described by the relationship of  $y = 1 - e^{-0.25x}$ .

A similar evaluation of the rate of cellulose degradation as was performed for the rates of lignin removal also shows a linear relationship between the increase in cellulose chain scission  $\Delta(1/DP)$  and the square root of ozonation time during the initial regime of ozonation (see Figure 5.5).

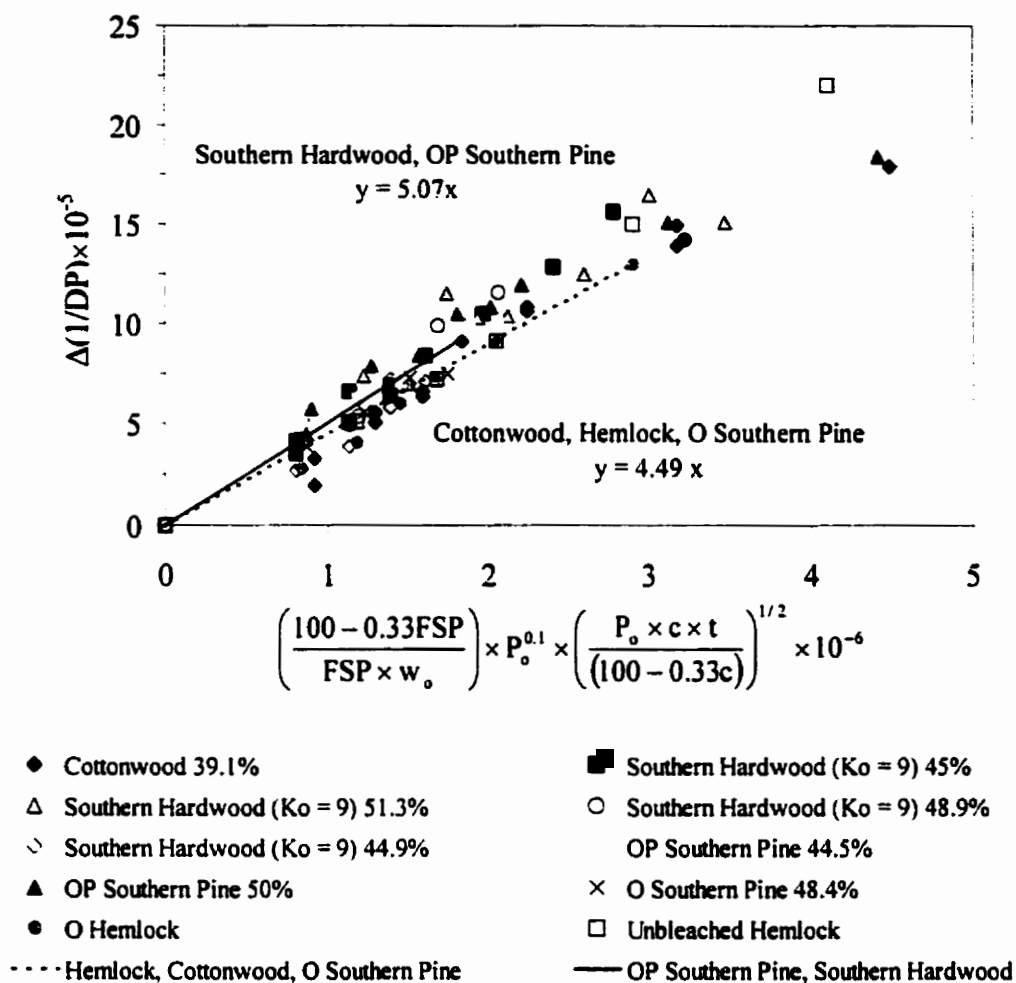


**Figure 5.5** Generalized curve of cellulose degradation.

Upon evaluating the trends of the generalized cellulose degradation data it is apparent that southern hardwood and OP southern pine degrade at a faster rate than the other pulps. The initial linear region of Figure 5.5 represents cellulose degradation during the initial regime of ozonation. The slope of the two straight lines correlations for the two groups of pulps in Figure 5.5 corresponds to  $\beta'$  of Equation 5.10. Contrary to the generalized delignification, the generalized cellulose degradation does not slow down

after the initial regime, because the direct attack by ozone on cellulose continues after the radical attack stops when all the lignin is consumed.

## 5.6 SELECTIVITY

The lignin-cellulose selectivity has traditionally been defined as the decrease in kappa number per unit viscosity loss,  $\Delta K / \Delta \text{Viscosity}$ . However, with the introduction of the generalized curves of delignification and cellulose degradation it is possible to account for the effect of initial lignin content and operating conditions on the selectivity by defining the generalized selectivity as;

$$\frac{\Delta K}{\frac{(\Delta K)_{\text{Lumen}}}{\Delta \left( \frac{1}{DP} \right)}} \times K_o^{0.5} \times P_o^{0.1} \quad (5.18)$$

The generalized selectivity for all of the pulps of this study is plotted in Figure 5.6 versus the fractional degree of delignification during the initial regime,  $\Delta K / (\Delta K)_{\text{Lumen}}$ . From Figure 5.6 it is evident that the lignin-carbohydrate selectivity decreases as the delignification increases beyond the initial regime, i.e.  $\Delta K / (\Delta K)_{\text{Lumen}} \geq 1$ . Beyond the initial regime of ozonation the rate of delignification slows as an increasing number of fibres become delignified and the rate of cellulose degradation increases due to direct attack on cellulose by ozone, thereby decreasing the selectivity.

## 5.7 CONCLUSION

Generalized relationships have been developed to describe the rates of delignification and cellulose degradation using solely measurable quantities of the pulp.

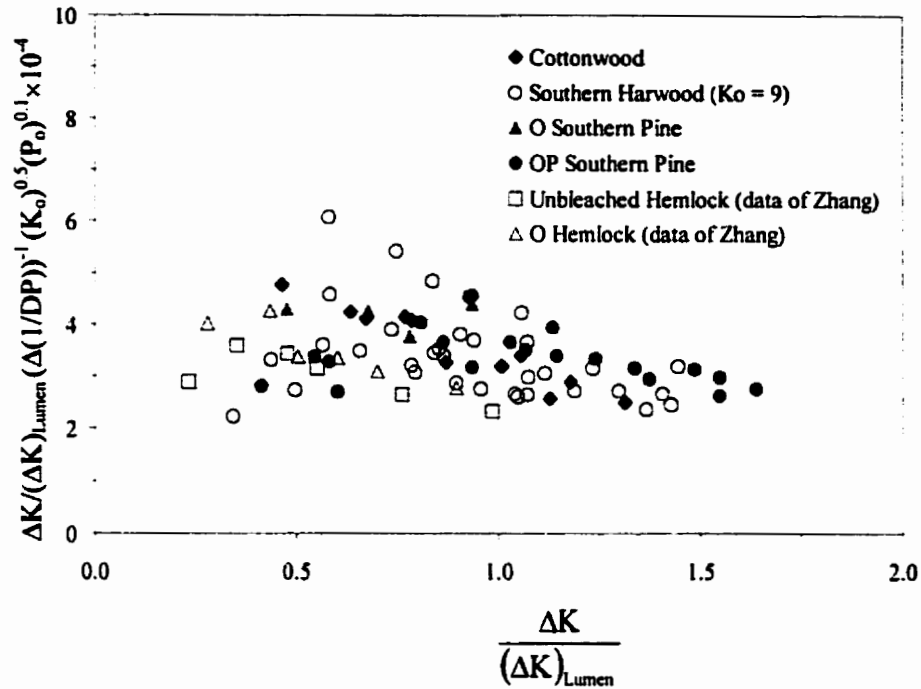


**Figure 5.6** Generalized selectivity for all pulp types.

By accounting for the physical parameters of the pulp fibres (FSP,  $w_o$ ,  $K_o$  and consistency) the initial regime of ozone delignification for each pulp type can be described by a common relationship of

$$\frac{\Delta K}{K_o} = 0.175 \left( \frac{100 - 0.33FSP}{FSP \times w_o} \right) \times \left( \frac{P_o \times c \times t}{K_o (100 - 0.33c)} \right)^{1/2} \times \frac{(\Delta K)_{Lumen}}{K_o} \quad (5.18)$$

with the exception of Hemlock pulp. Hemlock pulp has a lower rate of delignification than the other pulps studied.

Southern hardwood and OP southern pine degrade at a faster rate than the other pulps implying once again that the rate of cellulose degradation is somewhat dependent on the chemical nature of lignin. In agreement with the shrinking core model, the lignin-carbohydrate selectivity decreases beyond the initial regime of ozonation.

## **GENERAL CONCLUSIONS**

### **6.1 INTRODUCTION**

For optimum sizing of an ozone reactor for different pulp types, a fundamental understanding of the rate processes of delignification and cellulose degradation is needed. It has been shown [5] that the kinetics of pulp ozonation are governed by diffusion of ozone through the fibre wall and can be accurately described by the so called shrinking core model. Based on this model a quantitative description of the effect of ozone partial pressure, temperature and lignin content on the ozone bleaching kinetics has been proposed by Zhang [5] for Hemlock pulp. This thesis is concerned with applying this model to other pulp types and to expand the understanding by generalizing the rates of delignification and cellulose degradation in order to include the effect of species and consistency. In doing so, it was shown to be possible to predict the rates of delignification and cellulose degradation for any given pulp based on its chemical and physical characteristics and the applied ozonation conditions.

### **6.2 CONTRIBUTIONS TO KNOWLEDGE**

The theory of delignification and cellulose degradation as it is described by the shrinking core model, has been confirmed for five different pulp types. It has been shown for cottonwood, OP Southern Pine, O Southern Pine and Southern Hardwood of two different initial lignin contents and pre-ozonation treatment, that the rate of delignification and cellulose degradation is proportional to the square root of ozonation time during the initial regime of ozonation. After appropriate correction for initial kappa number,  $K_0$ , ozone partial pressure,  $P_o$ , fibre cell wall thickness,  $w_0$ , and fibre saturation

point, FSP, the delignification rate for hardwoods and softwoods are the same. This is consistent with the shrinking core model of delignification that requires the kinetics to be governed by diffusion of ozone in the fibre wall and not by lignin structure.

Although the rate of delignification is dependent solely on the physical state of the pulp fibres, the rate of cellulose degradation is also somewhat dependent on the chemical nature of the lignin structure. Pre-ozone treatment with peroxide results in an increased rate of cellulose degradation and a corresponding decrease in selectivity.

The rates of delignification and cellulose degradation are maximal at a consistency of about 10% above the fibre saturation point. The lignin-carbohydrate selectivity, however, is independent of pulp consistency within the experimental range.

It has been concluded that the optimum amount of lignin removal that can be achievable in a single ozone stage is approximately 50-60% of the initial lignin content. This optimum ozonation occurs as the ozone-lignin reaction front reaches the lumen of a significant number of pulp fibres, i.e. when the decrease in kappa number is equal to  $(\Delta K)_{\text{Lumen}}$ . A consistent method of determining  $w_o$  and therefore  $(\Delta K)_{\text{Lumen}}$  has been established based on the fibre width distribution curve.

With the determination of  $(\Delta K)_{\text{Lumen}}$  from the cumulative fibre wall width distribution, the rates of delignification and cellulose degradation can be related directly to solely measurable physical and chemical parameters (FSP,  $K_o$ ,  $w_o$ ,  $P_o$  and  $c$ ) of the ozone-pulp system. The developed generalized relationships for the decrease in kappa number and increase in cellulose chain scission are;

$$\frac{\Delta K}{K_o} = f_1 \left( \frac{100 - 0.33\text{FSP}}{\text{FSP} \times w_o} \right) \times \left( \frac{P_o \times c \times t}{K_o (100 - 0.33c)} \right)^{1/2} \times \frac{(\Delta K)_{\text{Lumen}}}{K_o}$$

$$\text{and } \Delta\left(\frac{1}{DP}\right) = f_2\left(\frac{100 - 0.33FSP}{FSP \times w_o}\right) \times P_o^{0.1} \times \left(\frac{P_o \times c \times t}{(100 - 0.33c)}\right)^{1/2}$$

where  $f_1$  and  $f_2$  are functions.

These relationships can be applied to any pulp type under low consistency, medium consistency or high consistency ozonation conditions.

It was confirmed that the predictive approach of Gandek[13] can be used to describe the initial regime of ozone delignification at the fibre saturation point of a new pulp based on solely on its initial lignin content and its average fibre wall thickness.

### 6.3 SUGGESTIONS FOR FUTURE WORK

1. It was found that hydrogen peroxide pre-treatment led to increased cellulose degradation. This effect was explained by an increased hydroxyl radical yield when lignin with  $\alpha$ -carbonyl groups is ozonated. Therefore it is suggested to study the kinetics of cellulose degradation during ozonation of fully bleached pulp impregnated with different lignin model compounds.
2. The value of  $(\Delta K)_{\text{Lumen}} / K_o$  increases when the fibre wall width distribution is narrower. Therefore it is suggested to classify pulp samples according to their fibre wall width using centrifugation techniques, and then to confirm the delignification kinetics using the experimental techniques used in this thesis.



3. **The present experimental technique does not provide information about the stoichiometry of the amount of ozone consumed per kappa number removed. This information is of much practical importance because recent studies have shown that the stoichiometry is strongly influenced when ozonation (Z stage) is combined with chlorine dioxide treatment (D stage) in a sequential D/Z or Z/D stage. Therefore it is suggested to modify the present kinetics measurement technique so that the ozone-lignin stoichiometry can be determined.**
4. **Measure the ozonation kinetics in (D/Z)E, (Z/D)E and (D/Z/D)E sequences which leads to high replacement ratios of chlorine dioxide by ozone (up to 4 kg ClO<sub>2</sub> by 1 kg O<sub>3</sub>).**
5. **Measure the effect of post-ozone treatment on the delignification and cellulose degradation kinetics. As particular post-ozone treatment one could consider application of peracetic acid ((Z/Paa)E), and chlorine dioxide ((Z/D) or ZED or ZND, with N being neutralization).**
6. **Investigate the effect of additives to improve the lignin-cellulose selectivity of ozone bleaching.**

## APPENDIX A CELL THICKNESS AND FIBRE DIAMETER DISTRIBUTIONS

(As determined by Econotech Services Ltd.)

Table A.1: cell wall thickness and fibre diameter distribution

Pulp Type	Cell wall thickness (S.D.) ( $\mu\text{m}$ )	Cell Diameter (S.D.) ( $\mu\text{m}$ )
Southern Hardwood ( $K_0=6$ )	5.3 (1.5)	20.0 (5.4)
Southern Hardwood ( $K_0=9$ )	5.1 (1.8)	19.4 (4.8)
Cottonwood	4.1 (1.1)	26.4 (5.7)
Unbleached Hemlock	4.6 (1.5)	42.1 (13.7)
O Southern Pine	5.7 (2.8)	41.7 (11.6)
OP Southern Pine	5.7 (2.7)	42.4 (12.8)

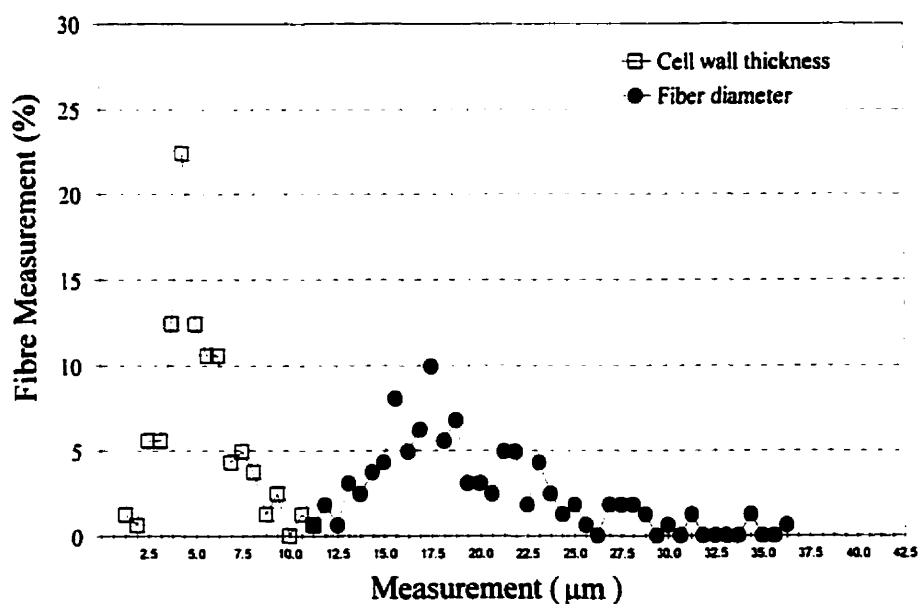


Figure A.1. Southern Hardwood ( $K_0=6$ )

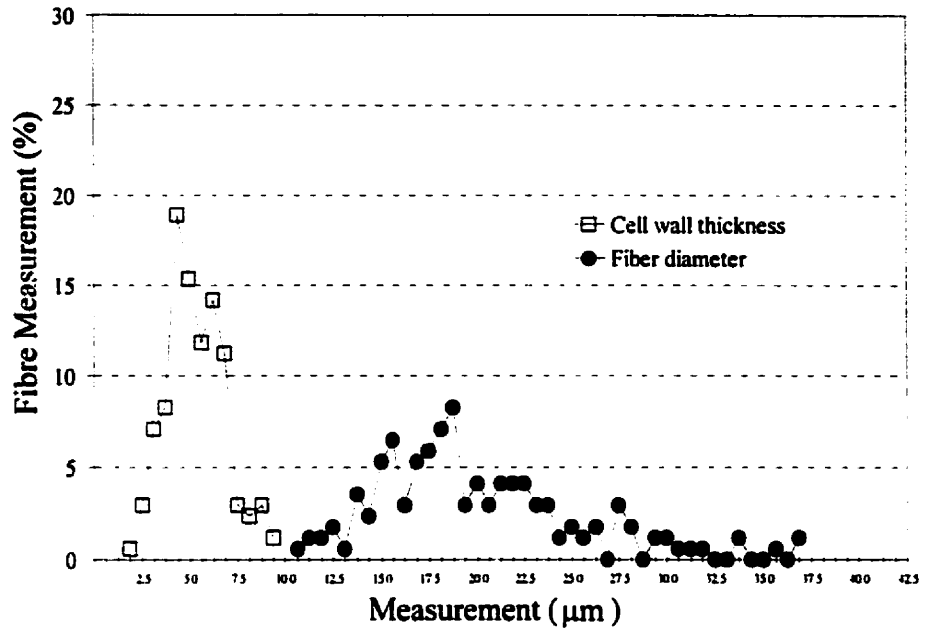


Figure A.2. Southern Hardwood ( $K_0=9$ )

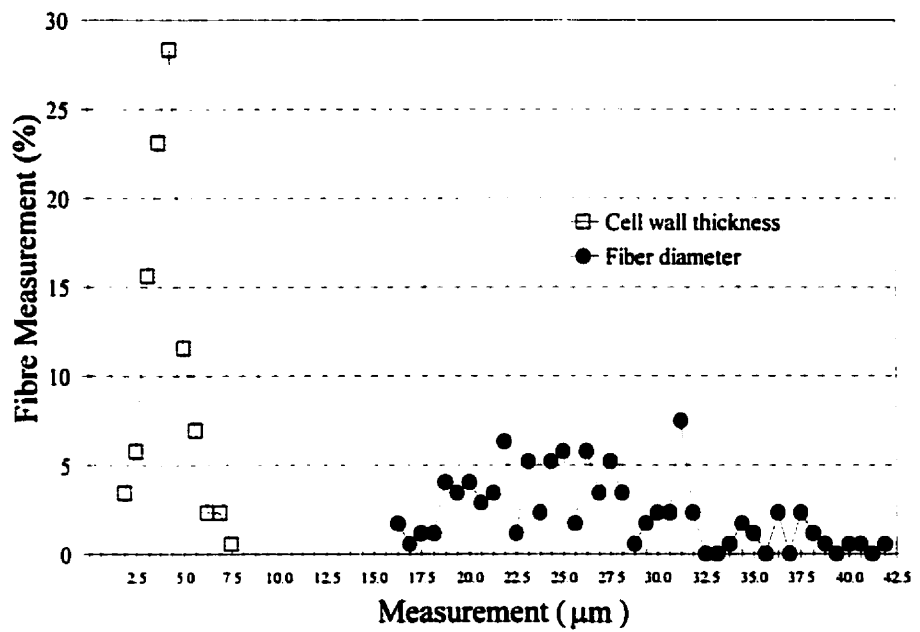


Figure A.3. Cottonwood

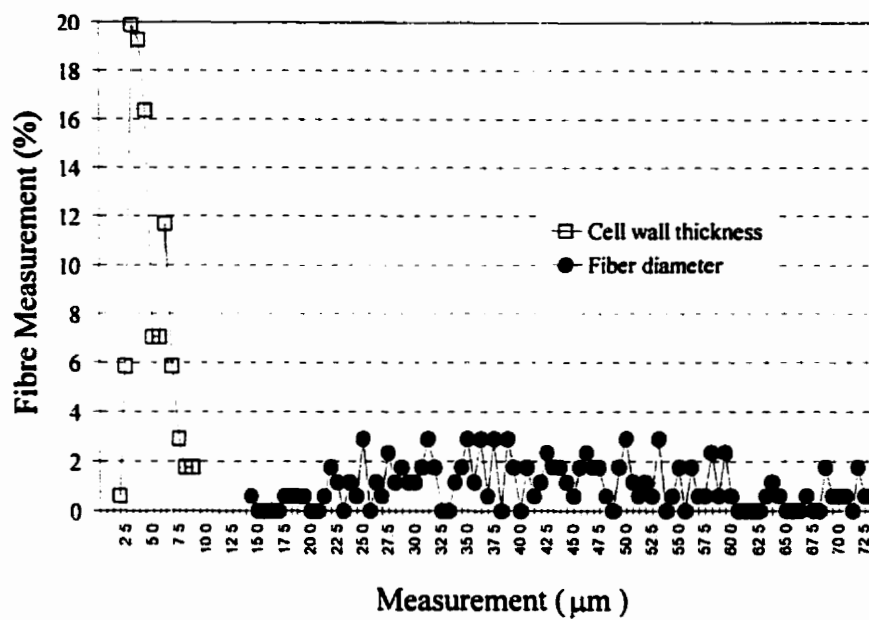


Figure A.4. Unbleached Hemlock

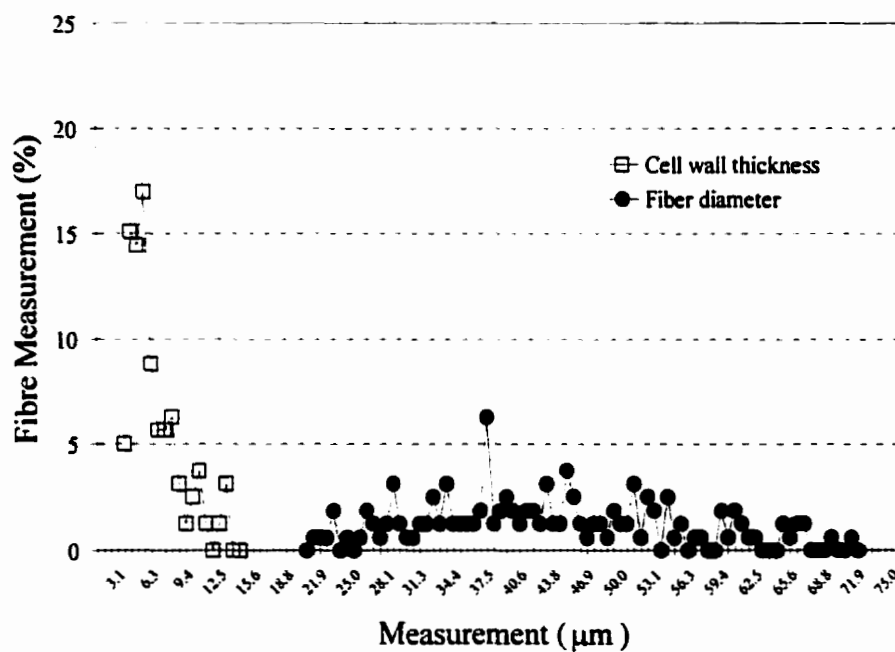


Figure A.5. O Southern Pine

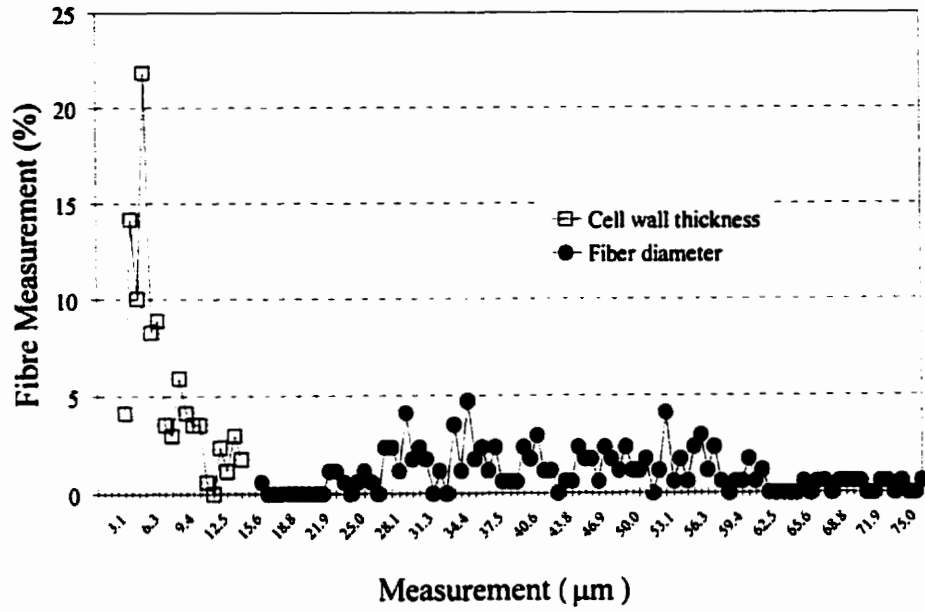


Figure A.6. OP Southern Pine

## **APPENDIX B PULP AND PAPER TERMINOLOGY**

**Viscosity** - A chemical test to quantify the cellulosic portion of chemical pulps by dissolving the pulp in a solvent and measuring the viscosity of the pulp solution. The viscosity of the solution gives an indication of the degree of polymerisation of the cellulose which is an indication of the degradation (or decrease in cellulose molecular weight) resulting from the pulping and/or bleaching processes.

**Consistency** - A measure of the dry fibre content of a pulp suspension defined as the ratio of the dry fibre mass to the mass of the pulp suspension. Consistency is expressed as a percentage.

**DP** - The degree of polymerisation refers to the number of repeating sugar units of a cellulose chain.

**Fibre Saturation Point, FSP** - The consistency at which a pulp fibre contains the maximum amount of water possible with no excess water on the outer surface of the fibre.

**Kappa Number, K** - A chemical test to determine the lignin content of chemical pulps. A carefully weighed pulp sample reacts with a known volume of permanganate solution under controlled conditions and the amount consumed is determined by

back-titration. The kappa number has a linear relationship with lignin content for pulps below 70% yield.

**REFERENCES**

- [1] Zhang, Y., G.J Kang, Y. Ni and A.R.P. van Heiningen, "Degradation of wood polysaccharide model compounds during ozone treatment", *JPPS* 23(1): J23-J27 (1997).
- [2] Kang, G.J., Y. Zhang, Y. Ni and A.R.P. van Heiningen, "Influence of lignin on the degradation of cellulose during ozone treatment", *J. Wood Chem. and Tech.* 15(4): 413-430 (1995).
- [3] White, D.E., T.P. Gandek, M.A. Pikulin, and W.H. Friend, "Importance of Reactor Design in High Consistency Ozone Bleaching", *Pulp and Paper Canada*, 94(9): 16-21 (1993).
- [4] Griffin, R., Y. Ni and A.R.P. van Heiningen, "The development of delignification and lignin-cellulose selectivity during ozone bleaching", *CPPA 81<sup>st</sup> Annual Meeting*, A117-A122 (1995).
- [5] Zhang, X.Z., "Ozone bleaching of chemical pulp", Ph.D. Thesis. University of New Brunswick, Department of Chemical Engineering (1997).
- [6] Pulliam, T, " Mills draw from a growing number of non-chlorine, TCF options" *Pulp & Paper* 69(9): 75-83 (1995).
- [7] Liebergott, N., B. van Lierop and A. Skothos, "A survey of the use of ozone in bleach pulps, part 1", *Tappi J.* 75(1): 145-152(1992).
- [8] Dence, C.W. and D.W. Reeve "Pulp bleaching, principles and practice", TAPPI Press, Atlanta, Georgia (1996).
- [9] Gandek, T.P., "Rate processes and uniformity in commercial high consistency ozone bleaching", *Intern. Pulp Bleaching Conf.*, Book 1:127-137, Helsinki, Finland (1998).
- [10] Nutt, W.E., S.W. Eachus and B.F. Gribbs, "Development of ozone Bleaching Process", *TAPPI 1992 Pulping Conf.*, Book 3: i 109-1026, Boston (1992).
- [11] Gottlieb, P.M., et al. "Mill experience in high-consistency ozone bleaching of southern pine pulp", *Tappi J.* 77(6):117-124 (1994).
- [12] Ruthkowski, J., "Environmentally friendly pulp bleaching technologies", *Cellulose Chem. Tech.* 31(5/6):485-497 (1997).
- [13] Bennington, C.P.J., X-Z Zhang and A.R.P. van Heiningen, "The effect of fibre width distribution on ozone bleaching", *JPPS* 25(4): 124-129 (1999).
- [14] Zhang, Y., G.J Kang, Y. Ni and A.R.P. van Heiningen, A. Mislankar, A. Darbie,



- and D. Reeve, "Initial delignification and cellulose degradation of conventional and ethanol assisted ozonation", *J. Wood Chem. and Tech.* 18(2): 129-157 (1998).
- [15] Levenspiel, O., "Chemical Reaction Engineering," New York: John Wiley & Sons, Inc., 2<sup>nd</sup> Edition (1972).
- [16] Zhang, X.Z., Y. Ni and A.R.P. vanHeiningen, "The prediction of the effect of operating variables on the rates of delignification and cellulose degradation during ozone bleaching", *Proc. Tappi Pulping Conf.*, pp331-349, Montreal (1998).
- [17] Ragnar, M., T. Eriksson and T. Reitberger, "The initial hydroxyl radical yield in reactions of ozone with lignin and carbohydrate model compounds, a kinetics study", *Proc. ISWPC*, A5, 1997.
- [18] Ragnar, M., T. Eriksson and T. Reitberger, "Superoxide- the initial radical in ozone bleaching", 5<sup>th</sup> European Workshop on Lignocellulosics and Pulp pp 555-558, Portugal (1998).
- [19] Zhang, X.Z., Y. Ni and A.R.P. vanHeiningen, "Kinetics of cellulose degradation during ozone bleaching", *Proceedings 85<sup>th</sup> Annual Meeting, PAPTAC*, A307-313, Montreal (1999).
- [20] Kerr, A.J. and D.A.S. Goring, "The ultrastructural arrangement of the wood cell wall", *Cellulose Chem. Tech.* 9:563-573 (1975).
- [21] Page, and de Grâce, "The delamination of fibre walls by beating and refining", *Tappi J.* 50(10): 489-495 (1967).
- [22] Scallan, A.M., "The structure of the cell wall of wood –A consequence of anisotropic inter-microfibrillar bonding?", *Wood Science* 6(3) 266-271 (1974).
- [23] Bailey, I.W. *Ind. Eng. Chem.* 30:40-47.
- [24] Zhang, X.Z., Y. Ni and A.R.P. van Heiningen, "Effect of consistency on chemical pulp ozonation: Calculation of the capillary cross-sectional area (ECCSA) and tortuosity ( $\lambda$ ) of the fibre wall", *Proc. 5<sup>th</sup> European Workshop on Lignocellulosics and Pulp*, pp 413-416, Portugal (1998).
- [25] Osawa, Z. and C. Schuerch, "The action of gaseous reactions on cellulose material, 1. Ozone and reduction of unbleached kraft pulp" and 2. "Pulping of wood with ozone", *Tappi J.* 46(2): 79-88 (1963).
- [26] Secrist, R.B., and R.P. Singh, "Kraft pulp bleaching II. Studies on ozonation of chemical pulps", *Tappi J.* 54(4) 581-584 (1971).

- [27] Zhang, Y., G.J Kang, Y. Ni and A.R.P. van Heiningen, "Kinetics of carbohydrate degradation due to direct attack by ozone", Presented at ISWPC, Montreal. (1997).
- [28] TAPPI Test Methods 1994-1995, TAPPI Press, Atlanta, Georgia (1994).
- [29] Scallan, A.M. and J.E. Carles, "The correlation of the water retention value with the fibre saturation point", Svensk Papperstidning Nr 17 30(9): 699-703 (1972).
- [30] Kamishima, T.F. and Akamastu, "Bleachability of softwood and hardwood draft pulps in ozone bleaching", Japan Tappi 30(7): 381-391 (1976).
- [31] Liebergott, N and B. van Lierop, "Ozone delignification of black spruce and hardwood kraft, kraft-anthraquinone pulps," Tappi J. 64(6):95-99 (1981).
- [32] Lindholm, C-A, "Effect of pulp consistency and pH in ozone bleaching, Part 3: Bleaching of oxygen delignified kraft pulp", Nordic Pulp Paper Res. J. 3(1):44-50 (1988).